

CLIP’s Visual Embedding Projector is a Few-shot Cornucopia

Mohammad Fahes¹ Tuan-Hung Vu^{1,2} Andrei Bursuc^{1,2} Patrick Pérez³ Raoul de Charette¹
¹ Inria ² Valeo.ai ³ Kyutai

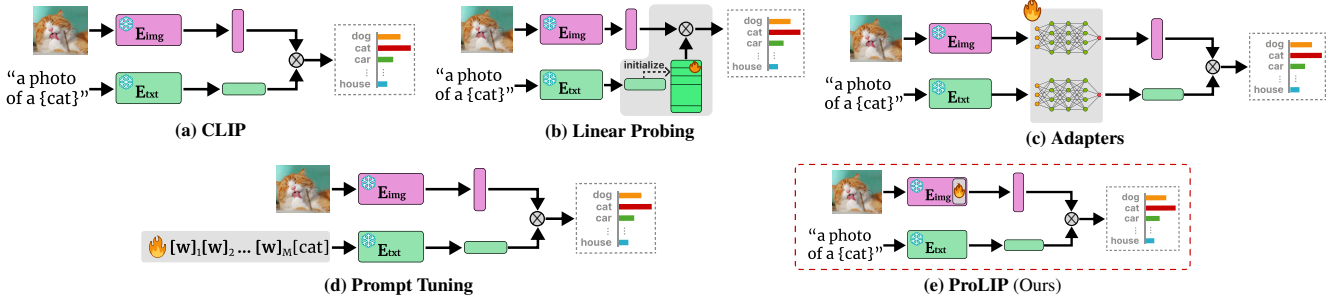


Figure 1. **Few-shot classification with CLIP.** (a) Using a pre-trained CLIP, *zero-shot* classification is performed by measuring text and visual embeddings similarity. Among *few-shot* adaptation strategies of CLIP, (b) Linear Probing [23, 42] trains a linear classifier of the visual features, (c) Adapters add external learnable MLPs [13, 58], (d) Prompt Tuning learns word embeddings [6, 62–64]. Alternatively, we propose (e) ProLIP which does not introduce new weights and only fine-tunes the visual embedding linear projector.

Abstract

We introduce ProLIP, a simple and architecture-agnostic method for adapting contrastively pretrained vision-language models, such as CLIP [36], to few-shot classification. ProLIP fine-tunes the vision encoder’s projection matrix with Frobenius norm regularization on its deviation from the pretrained weights. It achieves state-of-the-art performance on 11 few-shot classification benchmarks under both “few-shot validation” [23] and “validation-free” [42] settings. Moreover, by rethinking the non-linear CLIP-Adapter [13] through ProLIP’s lens, we design a Regularized Linear Adapter (RLA) that performs better, requires no hyperparameter tuning, is less sensitive to learning rate values, and offers an alternative to ProLIP in black-box scenarios where model weights are inaccessible. Beyond few-shot classification, ProLIP excels in cross-dataset transfer, domain generalization, base-to-new class generalization, and test-time adaptation—where it outperforms prompt tuning while being an order of magnitude faster to train. Code is available at <https://github.com/astravision/ProLIP>.

1. Introduction

Contrastive Language-Image Pretraining (CLIP) [36] has shown that contrastive learning at scale from noisy image descriptions yields strong visual features. CLIP’s visual-language space allows for a wide range of text-image down-

stream tasks, including in zero-shot settings.

At inference, CLIP performs zero-shot classification by measuring the similarity between image embeddings and class labels expressed as text prompts, as shown in Fig. 1a. Yet, the performance may still be unsatisfying for data underrepresented in CLIP’s pretraining set. Examples of such cases include geospatial data, *e.g.*, EuroSAT [18] and specialized data, *e.g.*, FGVCAircraft [32]. This has led to a key challenge in transfer learning: *how to efficiently adapt CLIP to new tasks with only a few labeled samples?*

Using only a few labeled samples, model training risks overfitting. The common strategy is to avoid full fine-tuning and instead adapt only a few parameters [29]. Starting from a concept-rich pretrained CLIP model, such parameter-efficient strategies have proved effective for few-shot tasks. To this end, the literature explores three avenues (Fig. 1). First, linear probing (LP) [23, 36, 42] trains a linear classifier on the frozen visual features. Second, Adapters [13, 43, 58] introduce a multi-layer perceptron (MLP) on top of frozen visual or text features, using residual connections to incorporate zero-shot features. Third, prompt tuning [62, 63] replaces the prompt template with learnable parameters, while freezing both vision and text encoders.

While simple and parameter-efficient, existing CLIP adaptation strategies come with important drawbacks. Linear probing [23, 31, 36, 42], cache-based adapters [58] and text adapters [53] are limited to few-shot settings and cannot handle open-class or cross-dataset tasks. Prompt tuning methods [6, 25, 62–64] are slow to train because gradients

must flow through the full text encoder; their performance can also fluctuate with context length and class-name positions. Adapter-based approaches [13, 43, 58] introduce architectural and hyperparameter sensitivity that complicates robust deployment across datasets.

Compounding these pitfalls, many prior CLIP few-shot adaptation methods also depend on per-dataset validation sets to tune critical hyperparameters [13, 14, 31, 53, 58], which conflicts with the spirit of the few-shot setting and undermines the goal of a single, universal configuration. For example, cache-based models [14, 58] typically rely on validation data to choose the cache-logit mixing weight and the scale of intra-modal distance. Recent analyses [23, 42] underscore how brittle this practice is: performance drops when hyperparameters are selected under *few-shot validation* [23] and degrades even more sharply under fully *validation-free* conditions [42].

In this paper, we propose a new method for CLIP adaptation, coined ProLIP. Our approach is simple to implement, requiring only a few lines of code and is highly effective. It fine-tunes the embedding projection matrix of the vision encoder (which maps visual embeddings into the shared vision-text space) using a cross-entropy loss, while regularizing it to stay close to the pretrained one using the Frobenius norm of their difference. ProLIP is a competitive baseline and is robust to variations in training configuration.

ProLIP offers major advantages:

- It requires no external parameters, eliminating the need for complex architecture searches and hyperparameter tuning. In the *validation-free* [42] setting, it maintains stable performance across learning rates by inversely scaling the regularization loss with the number of support samples per class.
- While other methods that fine-tune model weights are limited to ViTs [25, 26, 55], ProLIP works for both CNNs and ViTs.
- Fine-tuning only the projection matrix is highly efficient, taking only 2 seconds on saved pre-projected features.
- It retains CLIP’s open-class capability by using native text embeddings as classification weights, unlike [23, 31, 42, 53, 58] that constrain the classifier to a fixed label set.
- Its principle of regularized linear adaptation enables a simplified CLIP-Adapter [13] variant, Regularized Linear Adapter (RLA), which outperforms the original without requiring residual connection and architecture choices.

In experiments, ProLIP performs better or on par when compared to existing methods for few-shot classification, cross-dataset generalization, domain generalization, and base-to-new class generalization. It also significantly outperforms prompt tuning in test-time adaptation, while being one order of magnitude faster to train. Further, ProLIP generalizes seamlessly to other CLIP-like models such as SigLIP [56], leading to similar gains.

2. Related work

Parameter-efficient fine-tuning (PEFT). The advent of increasingly larger pretrained vision foundation models with strong generalization enables transfer learning approaches using limited labeled data. Full fine-tuning is computationally expensive and often underperforms even when compared to linear probing [29, 50]. PEFT methods adapt models with minimal parameter updates. Side-tuning [57] trains a small parallel network to prevent catastrophic forgetting. Optimizing specific parameters, like bias terms [54], is also effective but still requires full backpropagation. Adapter-tuning methods add adaptation modules to transformer blocks [21, 39], but incur higher runtime costs. LoRA [22] optimizes low-rank matrices in transformer layers to approximate weight changes, significantly reducing the number of parameters to learn. Prompt-tuning, such as VPT [24], adds learnable prompts to input patch embeddings. However, these methods are tailored for transformers and do not directly apply to convolutional networks.

Few-shot CLIP adaptation. Inspired by prompt tuning in NLP [30, 61], Zhou *et al.* [63] introduced context optimization (CoOp) for vision-language models, but it struggles to generalize to unseen classes. To address this, CoCoOp [62] adds a meta-network to generate input-conditional tokens, reducing overfitting to seen classes. Zhu *et al.* [64] noted that unconstrained prompt tuning can overfit in low-shot settings, harming zero-shot performance, and proposed regularizing training by updating only prompts aligned with zero-shot predictions. PLOT [6] uses optimal transport to match text and visual features, while MaPLe [25] learns prompts at both input and intermediate layers in vision and text branches with a coupling function.

An alternative to prompt tuning is training a linear probe on top of visual features [36]. Lin *et al.* [31] show that adding text descriptions to the training data improves linear probing, while Huang *et al.* [23] blend text embeddings with class-wise learnable classification weights.

Instead of prompt learning or linear probing, CLIP-Adapter [13] adds an MLP on top of the latent features, with a residual connection to preserve pretrained knowledge. Zhang *et al.* [58] propose a training-free cache-model, converting visual features from the few-shot set into MLP weights. Also training-free, Wang *et al.* [49] ensembles zero-shot classifiers with Gaussian Discriminative Analysis (GDA) [2], assuming Gaussian-distributed class features. CLIPoold [41] fine-tunes the full encoder with beta moving average regularization to maintain similarity to zero-shot weights. Notably, we only fine-tune the embedding projector, using 0.45% of the parameters compared to CLIPoold and a simpler regularization. Recently, Zanella *et al.* [55] showed that applying LoRA [22] to CLIP improves few-shot classification performance, but the method is ViT-

specific and causes new class knowledge forgetting [11].

Some works leverage external priors to boost few-shot performance. For instance, APE [66] uses GPT-3 to generate descriptions, CaFo [59] uses GPT-3 [4], DINO [5], and DALL-E [37], while AMU-tuning [45] presents a unified perspective on few-shot adaptation strategies from a logit bias perspective and uses MoCov3 [7] as additional prior. Our work belongs to the category harnessing only the CLIP model with no extra information [23, 25, 42, 53, 58].

3. ProLIP

CLIP’s visual encoder outputs latent visual features, which are then linearly projected into the shared vision-text latent space by a learned linear layer, *i.e.*, visual embedding projector. Thus, the vision encoder f can be written as $f = f_2 \circ f_1$, where f_2 represents the linear projection head, and f_1 represents all the preceding layers. Given an image \mathbf{l} , this writes:

$$\mathbf{x}_o = f_1(\mathbf{l}), \quad \mathbf{v} = f_2(\mathbf{x}_o) = \mathbf{W}_o \mathbf{x}_o + \mathbf{b}_o, \quad (1)$$

with $\mathbf{x}_o \in \mathbb{R}^{D_o}$ the latent visual features before projection, $\mathbf{W}_o \in \mathbb{R}^{D \times D_o}$ the projection matrix and \mathbf{b}_o a bias term. We show that fine-tuning only the projection matrix \mathbf{W}_o in Eq. (1) can be a strong alternative to prompt tuning and feature adapters. Specifically, the probability that a sample i belongs to the class k is computed as the Softmax over cosine similarities of image-text embeddings:

$$p_{ik}(\mathbf{W}_o) = \frac{\exp((\mathbf{W}_o \mathbf{x}_{oi} + \mathbf{b}_o)^\top \mathbf{t}_k / \tau)}{\sum_{j=1}^K \exp((\mathbf{W}_o \mathbf{x}_{oi} + \mathbf{b}_o)^\top \mathbf{t}_j / \tau)}, \quad (2)$$

with \mathbf{t}_k being the fixed text representation of class k since the text encoder is frozen, τ the pretraining temperature parameter, $\mathbf{x}_{oi} = f_1(\mathbf{l}_i)$ the pre-projection embedding of sample i , and \mathbf{b}_o the frozen bias (0 for ViT backbone). The matrix \mathbf{W}_o is learned with gradient descent using a cross-entropy loss $L(\mathbf{W}_o)$:

$$L(\mathbf{W}_o) = -\frac{1}{NK} \sum_{i=1}^N \sum_{k=1}^K y_{ik} \log p_{ik}(\mathbf{W}_o), \quad (3)$$

where y_{ik} is the ground truth.

Regularization. Unconstrained fine-tuning can lead to forgetting the rich pretrained knowledge of CLIP. An effective fine-tuning strategy should therefore balance adaptation to the downstream task with preservation of the pretrained representations. Therefore, to prevent significant drift from the original weights (*i.e.*, knowledge forgetting), we add a regularization term based on the Frobenius norm of the difference between the pretrained and fine-tuned matrices. The total loss is:

$$L_{\text{ProLIP}} = L(\mathbf{W}_o) + \lambda \|\mathbf{W}_o - \mathbf{W}_o^{(0)}\|_F^2, \quad (4)$$

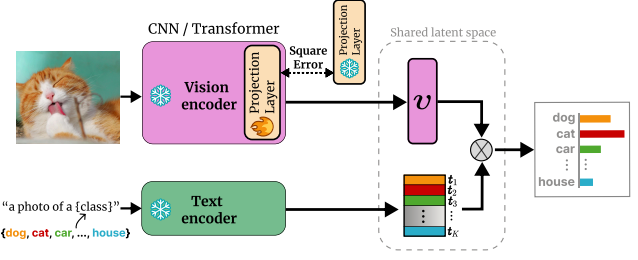


Figure 2. **ProLIP for few-shot adaptation.** Whether the vision encoder is a CNN or a Transformer, ProLIP trains only the layer that projects the visual embeddings into the shared latent space. The text encoder is frozen, and the text embeddings of the K target concepts are used as classification weights. Training with cross-entropy is regularized by a squared error loss ensuring weights of the projection layer to remain close to pretrained ones.

where $\mathbf{W}_o^{(0)}$ denotes the pretrained value of \mathbf{W}_o .

λ as a function of N . We later show that setting λ as a decreasing function of the number N of shots per class (*e.g.*, $\lambda = 1/N$ or $\lambda = 1/N^2$) helps mitigate overfitting while crucially stabilizing performance across a wide range of learning rates. Such observation corroborates classical findings in statistical learning since overfitting risk is known to increase with fewer data points [16]. Intuitively, in data-scarce settings (*e.g.*, $N = 1$), we want to rely more on the zero-shot model for classification by increasing λ , and when data increases (*e.g.*, $N = 16$) we allow the model to learn more from data by decreasing λ . From learning-theoretic standpoint, this scaling is consistent with generalization bounds where the effective complexity term decreases as N increases [1]. An overview of ProLIP is shown in Fig. 2.

Of note, we are not the first to propose minimizing Frobenius norm as regularization strategy. Such regularization is commonly used to avoid forgetting [15, 27]. However, the framework proposed by Gouk *et al.* [15] is generic and consists of regularized fine-tuning of the model weights across layers, which contradicts PEFT and is shown later in the experimental section to be less effective. ProLIP revisits this idea for the projection matrix with a new N -dependent regularization weight λ to stabilize few-shot adaptation and preserve zero-shot capability of CLIP. To our knowledge, our strategy has not been done in CLIP adaptation, and offers a stronger and simpler alternative to complex methods.

ProLIP can be applied on pre-processed data (*i.e.*, saved pre-projection features), which makes it extremely fast to train. A PyTorch-like [35] pseudo-code for ProLIP is provided in supplementary material.

A logit bias perspective on ProLIP. Recently, Tang *et al.* [45] proposed interpreting CLIP few-shot adaptation methods from a unified perspective of logit bias. That is, every method learns a bias on top of the zero-shot CLIP logits.

For instance, the bias learned by TaskRes [53] is a new linear probe trained on top of frozen visual features \mathbf{v} . Another example is Tip-Adapter-F [58] where the learned bias is based on intra-modal similarity measures. For ProLIP, we fine-tune the projection matrix \mathbf{W}_o . Omitting \mathbf{b}_o for simplicity, the logits can be written as:

$$\text{Logits}_{\text{ProLIP}} = \mathbf{x}_o^\top \mathbf{W}_o^\top \mathbf{t} = \mathbf{x}_o^\top \mathbf{W}_o^{(0)\top} \mathbf{t} + \mathbf{x}_o^\top \mathbf{B}^\top \mathbf{t}. \quad (5)$$

That is, fine-tuning \mathbf{W}_o is equivalent to learning a matrix \mathbf{B} , initialized with $\mathbf{0}_{D \times D_o}$. Thus, the bias learned by ProLIP is a linear combination of the pre-projected features, trained to match the fixed text-based probe \mathbf{t} .

We show in the experiments that these different biases can be complementary, which suggests that they contain orthogonal knowledge learned during few-shot adaptation.

4. Revisiting CLIP-Adapter with ProLIP’s principles: Regularized Linear Adapter

ProLIP fine-tunes a *linear transformation* of pre-projected features, starting from a zero-shot model as the *initialization*, while *regularizing* the weights to stay close to their original values. We revisit here CLIP-Adapter with ProLIP’s principles, leading to Regularized Linear Adapter (RLA) which serves as an alternative to ProLIP in black-box model scenarios.

CLIP-Adapter. CLIP-Adapter learns a randomly initialized MLP $h_\theta(\cdot)$ on top of the frozen vision encoder using a residual connection α . The probability that a sample i belongs to the class k in this case writes:

$$p_{ik}(\theta) = \frac{\exp((\alpha \mathbf{v}^\top + (1 - \alpha)[h_\theta(\mathbf{v})]^\top) \mathbf{t}_k / \tau)}{\sum_{j=1}^K \exp((\alpha \mathbf{v}^\top + (1 - \alpha)[h_\theta(\mathbf{v})]^\top) \mathbf{t}_j / \tau)}, \quad (6)$$

where $h_\theta(\mathbf{v}) = \text{RELU}(\mathbf{W}_2 \text{RELU}(\mathbf{W}_1 \mathbf{v}))$, $\mathbf{W}_1 \in \mathbb{R}^{D/B \times D}$ and $\mathbf{W}_2 \in \mathbb{R}^{D \times D/B}$ being the two layers, B the bottleneck dimension and $\text{RELU}(x) = \max(0, x)$ the activation.

This formulation includes not only the learning rate but also two additional hyperparameters, α and B , along with architectural choices such as the number of layers and activation function. This makes the training impractical, as it requires a validation set to select these hyperparameters, which increases computational time. We later corroborate this performance sensitivity in the experimental section through 13 200 runs of CLIP-Adapter.

Regularized Linear Adapter (RLA). We revisit CLIP-Adapter [13] and incorporate ProLIP’s principles by (i) replacing the non-linear MLP with a linear transformation, (ii) initializing it with the identity matrix instead of random weights, and (iii) regularizing it during training with Frobenius norm. This variant of CLIP-Adapter is called Regularized Linear Adapter (RLA). For RLA, the probability that a

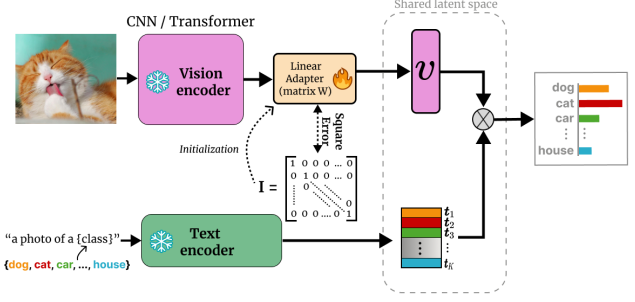


Figure 3. **Reglularized Linear Adapter (RLA).** RLA is a black-box version of ProLIP. Instead of fine-tuning the projection matrix, an external linear adapter is added and trained using cross-entropy loss, with squared-error regularization ensuring that the adapter’s weights remain close to the identity matrix.

sample i belongs to the class k writes:

$$p_{ik}(\mathbf{W}) = \frac{\exp(\mathbf{v}^\top \mathbf{W} \mathbf{t}_k / \tau)}{\sum_{j=1}^K \exp(\mathbf{v}^\top \mathbf{W} \mathbf{t}_j / \tau)}, \quad (7)$$

It can be seen from Eq. (7) that the linear adapter $\mathbf{W} \in \mathbb{R}^{D \times D}$ is multimodal by construction. Following the same principle of ProLIP, RLA is trained with cross-entropy loss $L(\mathbf{W})$ regularized with the Frobenius norm between the fine-tuned matrix \mathbf{W} and its initialization \mathbf{I} (the identity matrix). The total loss of RLA writes:

$$L_{\text{RLA}} = L(\mathbf{W}) + \lambda \|\mathbf{W} - \mathbf{I}\|_{\text{F}}^2, \quad (8)$$

RLA exhibits strong stability across learning rates when λ is inversely proportional to N , and outperforms the non-linear CLIP-Adapter, challenging the need for a bottleneck layer to learn new features [13]. An additional advantage of RLA is that it can substitute for ProLIP in black-box settings where the base model’s weights cannot be fine-tuned. RLA is illustrated in Fig. 3.

Conclusive remarks. ProLIP and RLA suggest CLIP’s representations already lie in a space where regularized linear transformations suffice to align features to new tasks. A prominent challenge in selective fine-tuning is choosing the set of parameters to tune for adaptation. Our work suggests that these parameters are not necessarily distributed across all the layers, therefore eliminating the need for backpropagation over the entire network [25, 55] and paving the way for more efficient adaptation of other multimodal foundation models.

5. Experiments

Datasets. Following prior CLIP few-shot learning work, we experimentally test ProLIP on 11 datasets for few-shot classification and base-to-new generalization: ImageNet [9], SUN397 [51], DTD [8], Caltech101 [12], UCF101 [44],

Method	# params	$N = 1$	2	4	8	16
CLIP (0-shot)		58.89				
<i>Prompt tuning</i>						
CoOp [63]	$K \times M \times D_e$	59.62 ± 3.11	63.80 ± 2.32	67.23 ± 1.64	71.30 ± 0.86	74.06 ± 0.55
PLOT [6]	$P \times K \times M \times D_e$	61.51 ± 2.91	65.67 ± 2.06	68.39 ± 1.17	71.96 ± 0.70	74.35 ± 0.66
KgCoOp [52]	$K \times M \times D_e$	61.36 ± 3.04	63.23 ± 2.06	65.73 ± 1.15	67.50 ± 1.11	69.01 ± 0.79
ProGrad [64]	$K \times M \times D_e$	62.46 ± 1.89	65.88 ± 1.46	68.52 ± 1.15	71.82 ± 0.11	73.95 ± 0.68
<i>Adapters</i>						
CLIP-Adapter [13]	$2(\bar{D}_B \times \bar{D})$	60.32 ± 0.80	61.93 ± 0.93	65.12 ± 0.80	69.20 ± 0.56	72.57 ± 0.54
Tip-Adapter-F [58]	$N \times K \times D$	61.29 ± 0.92	62.94 ± 0.75	66.02 ± 0.80	69.88 ± 0.51	73.82 ± 0.55
Tip-Adapter-F* [58]	$N \times K \times D$	63.06 ± 1.05	66.47 ± 0.65	68.71 ± 0.96	71.78 ± 1.00	74.37 ± 0.35
<i>Linear Probing</i>						
LP [36]	$K \times \bar{D}$	36.10 ± 1.43	46.99 ± 1.29	56.72 ± 1.20	64.66 ± 0.55	70.56 ± 0.44
LP++ [23]	$K \times (D+1)$	63.43 ± 0.90	66.20 ± 0.72	69.16 ± 0.79	72.04 ± 0.46	74.42 ± 0.45
<i>Model weights</i>						
ProLIP	$\bar{D}_o \times \bar{D}$	64.21 ± 1.93	67.43 ± 1.37	70.58 ± 1.08	73.73 ± 0.75	76.50 ± 0.50

Table 1. **Few-shot classification with few-shot validation.** We report the classification accuracy (%) averaged over 11 datasets and 10 seeds, comparing ProLIP to baselines taken from [23]. Note that baselines numbers differ from those reported in the original papers as they used a large validation set to tune hyperparameters. We highlight **best** and **2nd best**. First row provides zero-shot classification for reference. D_e is the dimension of the token embedding space, P the number of prompts in PLOT, M the context length, and D_B the bottleneck dimension of CLIP-Adapter.

Flowers102 [33], StanfordCars [28], FGVCAircraft [32], EuroSAT [18], OxfordPets [34] and Food101 [3]. For domain generalization experiments we follow ProGrad [64], using ImageNet as source dataset and testing on ImageNet-V2 [38], ImageNet-Sketch [48], ImageNet-A [20] and ImageNet-R [19] as out-of-distribution (OOD) datasets. For the cross-dataset transfer experiment, ProLIP is trained on ImageNet and evaluated on the other 10 datasets, similar to ProGrad [64]. For test-time adaptation, we use ImageNet and its OOD variants similarly to TPT [40].

Training details. Following prior work we use $N \in \{1, 2, 4, 8, 16\}$ shots as support training set for few-shot classification. For domain generalization and cross-dataset transfer experiments, we use $N=4$ like ProGrad [64]. For base-to-new generalization, we set $N=4$ like ProGrad [64] when using ResNet-50 (RN50) and $N=16$ like MaPLe [25] when using ViT-B/16. Unless otherwise stated, we employ ResNet-50 with CLIP weights as the visual encoder, similarly to the literature. Training runs for 300 epochs on a full-batch of features, taking up to 2s on one Tesla V100.

Baselines. We compare against a variety of existing adaptation strategies that harness only the CLIP model without using external pretrained networks. Among the baselines, we compare to *prompt learning* (e.g., CoOp [63], CoCoOp [62], PLOT [6], KgCoOp [52], ProGrad [64], MaPLe [25]), *adapters* (e.g., CLIP-adapter [13], Tip-adapter [58], TaskRes [53]), and *linear probing* methods (e.g., LP [36], LP++ [23], CLAP [42]). Note that, in

Sec. 5.1, Tip-adapter performance is reported in two settings following [23]: Tip-adapter-F where its two crucial hyperparameters are set to 1 and the validation set is used for early stopping, and Tip-adapter-F* where intensive hyperparameter search is performed to find the best values of the same hyperparameters based on the same validation set. More baselines are included in supplementary material.

Fair protocol for hyperparameter tuning. Different from the few-shot CLIP literature [58] relying on large validation sets for hyperparameter tuning, authors of LP++ [23] advocate for a few-shot validation set, *i.e.*, using a validation set with as many shots as in the training set. Going one step further, we argue that a truly realistic few-shot setting should not use *any* validation set as in [42]. For comparison purposes, in Sec. 5.1 we evaluate in the few-shot validation setting, but the core of our evaluation, from Sec. 5.2 onwards, focuses on the *validation-free setting*. Moreover, we evaluate ProLIP on 10 random seeds (*i.e.*, support training sets) for each dataset, as advised by Huang et al. [23].

For Sec. 5.1 only, the learning rate (LR) and regularizer loss weight λ are selected by grid search on the few-shot validation set, with $LR \in \{10^{-2}, 10^{-3}, 10^{-4}, 10^{-5}, 10^{-6}, 10^{-7}, 10^{-8}\}$ and $\lambda \in \{0, 1, 10^{-1}, 10^{-2}, 10^{-3}, 10^{-4}, 0\}$.

For Sec. 5.2 and following sections, having no access to a validation set, we show that using our regularizer ($\lambda > 0$) prevents severe overfitting, therefore allowing to set a fixed LR over all datasets, and a parametric λ as a decreasing

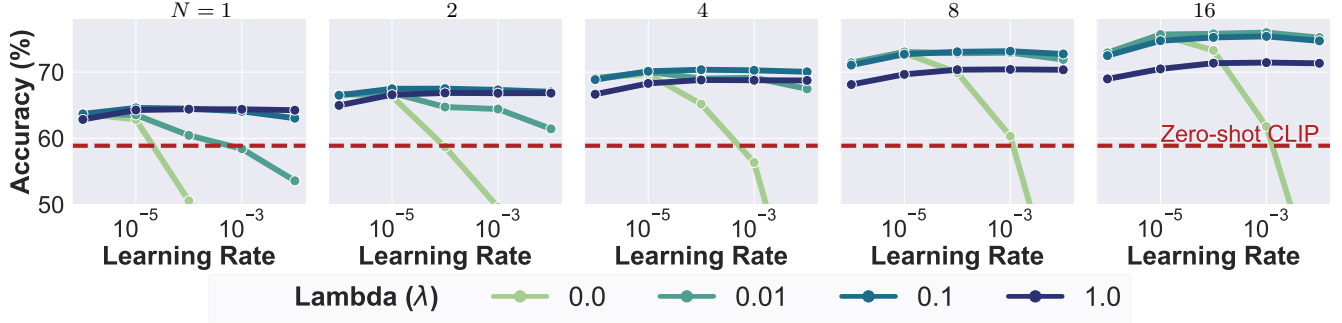
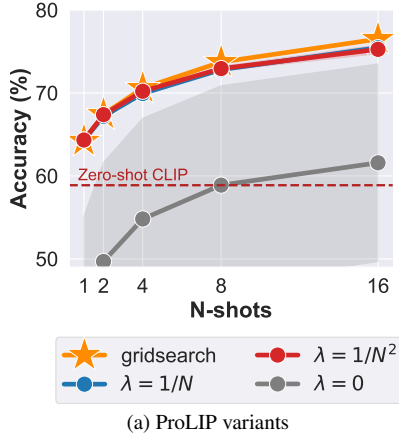


Figure 4. **ProLIP sensitivity to hyperparameter.** Accuracy of ProLIP as function of the hyperparameters (learning rate and regularization weight λ) for $N \in \{1, 2, 4, 8, 16\}$ -shot settings. Each data point is an average over 11 datasets and 10 seeds.



(a) ProLIP variants

Method	# params	$N = 1$	2	4	8	16
CLIP (0-shot)					58.89	
<i>Prompt tuning</i>						
ProGrad [64]	$K \times M \times D_e$	62.61	64.90	68.45	71.41	74.28
PLOT [6]	$P \times K \times M \times D_e$	62.59	65.23	68.60	71.23	73.94
<i>Adapters</i>						
TaskRes [53]	$K \times D$	61.44	65.26	68.35	71.66	74.42
Tip-Adapter-F [58]	$N \times K \times D$	60.29	62.26	65.32	68.35	71.40
<i>Linear Probing</i>						
Cross-modal LP [31]	$K \times D$	62.24	64.48	66.67	70.36	73.65
CLAP [42]	$K \times D$	62.79	66.07	69.13	72.08	74.57
<i>Model weights</i>						
ProLIP _∅	$D_o \times D$	64.33	67.19	69.94	72.82	75.46

(b) Few-shot without validation sets

Table 2. **Few-shot classification without validation set.** (a) ProLIP variants with performance averaged over 11 datasets, 10 seeds, and 4 learning rates $LR \in \{10^{-5}, 10^{-4}, 10^{-3}, 10^{-2}\}$ to study sensitivity. Note the low variance of the parametric formulations ($\lambda = 1/N$, $\lambda = 1/N^2$) which also reach the performance of the grid search variant — despite having no access to a validation set. (b) Comparison to validation-free baselines from [42] showing the consistent superiority of ProLIP_∅. Tab. 1 defines D_e , M & P .

function of the number N of shots.

5.1. Few-shot classification with few-shot validation

Tab. 1 reports the average classification accuracy across 11 datasets and 10 seeds. Per-dataset performances are in the supplementary material. In all few-shots settings (*i.e.*, $N \in \{1, 2, 4, 8, 16\}$), ProLIP clearly outperforms all the baselines, showing a great potential of the extremely simple approach of fine-tuning the visual embedding linear projector with regularization for adaptation.

Hyperparameters sensitivity. The regularization benefit of ProLIP is evident when tested with different hyperparameters fixed across datasets. Fig. 4 shows the average accuracy across the same 11 datasets for 4 different LRs, combined with regularization ($\lambda \in \{10^{-2}, 10^{-1}, 1\}$) or without ($\lambda=0$). When $\lambda=0$, accuracy drops dramatically at higher LRs due to overfitting on the few-shot training set, causing drift from the robust pretrained CLIP representation. In contrast, using weight regularization ($\lambda > 0$) reduces over-

fitting and LR sensitivity. This is supported by grid search statistics (see supp.), which show that the best LRs span a wide range. Our regularization thus mitigates overfitting, enabling the use of larger LRs (*e.g.*, 10^{-2}). This motivates our exploration of a more realistic setting where hyperparameters are not tuned, *i.e.*, *no validation data is used*.

5.2. Few-shot classification without validation set

An additional merit of ProLIP stems from its lower sensitivity to hyperparameters, as demonstrated in the previous section. It can be observed from Fig. 4 that for lower-shot settings, higher λ values lead to better accuracy, and vice versa. Therefore, we formulate λ as a decreasing function of the number of shots N , reporting in Tab. 2a the average performance over learning rates $LR \in \{10^{-5}, 10^{-4}, 10^{-3}, 10^{-2}\}$. It results that our simple parametric formulations of λ (*i.e.*, $1/N$, $1/N^2$) lead to almost identical, strong and stable results, competing with our state-of-the-art grid search variant, albeit without the need of a validation set. A byproduct of our regularizer is the reduced sensitivity to the learning

rate (*i.e.*, low variance as seen in Tab. 2a), whereas removing the regularizer (*i.e.*, $\lambda = 0$) proves to result in dramatically large variance. Detailed numbers for each combination are reported in the supplementary material. Therefore, in Tab. 2b we compare the average across 11 datasets of the validation-free baselines from [42], and the validation-free ProLIP variant, coined as ProLIP $_{\emptyset}$, with $\lambda = 1/N$ and average over the 4 tested learning rates. The reported performance shows a consistent improvement for any N .

In terms of parameters, depending on K and the used architecture, ProLIP can be more efficient than CLAP and vice versa. For example, ProLIP trains 393K/149M (0.0026%) parameters for ViT-B/16, while CLAP trains 512K/149M (0.0034%) for ImageNet and 51K/149M (0.00034%) for Caltech101, resulting in similar percentage range.

Comparison to architecture-specific baselines (*e.g.*, CLIP-LoRA [55], normalization techniques [47, 60]) is provided in the supplementary material.

5.3. Regularized Linear Adapter (RLA)

Fig. 5 illustrates the sensitivity of CLIP-Adapter to learning rate (LR) and residual weight (α) through **13 200 training runs** (11 datasets \times 10 seeds \times 5 settings \times 4 LRs \times α). Our RLA outperforms CLIP-adapter, showing stability across different LRs in the *validation-free* setting, though it still trails behind ProLIP $_{\emptyset}$. Detailed LR results are provided in the supplementary material. These findings reinforce the core principles of ProLIP and shed further light on why it is so effective, apart from the perhaps surprising effect of fine-tuning the visual embedding projector.

5.4. Generalization of few-shot models

Achieving generalization in a few-shot framework is challenging but crucial for evaluating the practical use of few-shot methods. We here explore three aspects of generalization: domain generalization, cross-dataset generalization and base-to-new generalization. Comparison is done only among the few-shot methods; the zero-shot CLIP performance is included as reference. For ProLIP $_{\emptyset}$, we systematically use $\lambda = 1/N$ and a fixed LR of 10^{-5} .

Cross-dataset generalization. Tab. 3 shows ProLIP $_{\emptyset}$ outperforms ProGrad on 6 out of 11 datasets, and on average, but zero-shot CLIP remains the strongest baseline. As argued in CoCoOp [62], training on ImageNet leads to good generalization to datasets like OxfordPets and Caltech101. However, for fine-grained or specialized datasets (*e.g.*, FGVC Aircraft, DTD), ProLIP $_{\emptyset}$ outperforms other methods but still lags behind zero-shot performance. Overall, ProLIP $_{\emptyset}$ retains the most zero-shot capability and shows better cross-dataset transferability.

Domain generalization (DG). In this setting, the set of classes is fixed in both in-domain and OOD datasets. Following ProGrad, we train ProLIP $_{\emptyset}$ on ImageNet (IN) as

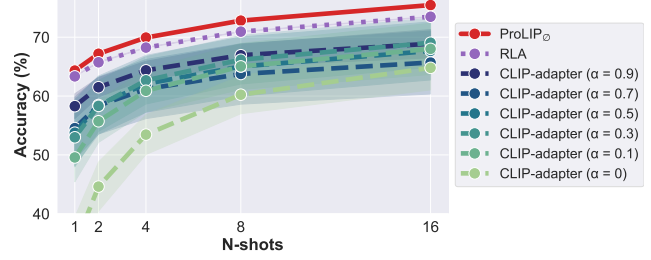


Figure 5. **Improving CLIP-Adapter with ProLIP’s principles** results in Regularized Linear Adapter (RLA) variant. We report classification accuracy (%) averaged over 11 datasets, 10 seeds, and 4 learning rates $LR \in \{10^{-5}, 10^{-4}, 10^{-3}, 10^{-2}\}$ for CLIP-Adapter with different α values, ProLIP $_{\emptyset}$ and RLA with $\lambda = 1/N$. Variance is halved for readability.

Method	Source		Target										Average
	ImageNet	Caltech101	OxfordPets	StanfordCars	Flowers102	Food101	FGVC Aircraft	SUN397	DTD	Eurosat	UCF101		
CLIP (0-shot)	60.35	85.84	85.75	55.78	65.98	77.35	17.07	58.85	42.69	36.22	61.80	58.88	
CoOp	61.34	84.48	85.99	54.16	60.10	75.48	14.09	57.48	35.32	26.72	57.56	55.70	
CoCoOp	61.04	84.73	86.42	52.34	61.24	73.79	13.74	55.94	36.60	23.46	57.97	55.21	
ProGrad	62.17	88.30	86.43	55.61	62.69	76.76	15.76	60.16	39.48	24.87	58.70	57.36	
ProLIP $_{\emptyset}$	62.55	86.99	84.00	54.19	64.03	74.95	16.99	59.67	41.09	36.55	60.95	58.36	

Table 3. **Cross-dataset generalization.** Training is performed on 4-shot ImageNet (source), except for ‘CLIP’ which is 0-shot. The learned models are evaluated on 10 other datasets (target). Baselines’ scores are average of 3 seeds reported from ProGrad [64].

source dataset (with $N=4$), and assess it on ImageNet-V2 (IN-V2), ImageNet-Sketch (IN-S), ImageNet-A (IN-A) and ImageNet-R (IN-R). Tab. 4 shows that ProLIP $_{\emptyset}$ is on par with or better than other methods on source and especially OOD domains, for both ResNet and ViT CLIP backbones. Of note, ProLIP $_{\emptyset}$ ’s performance stability across learning rates also applies for DG. For instance, with RN50, increasing LR to 10^{-2} results in an OOD accuracy drop of only -0.18% for ProLIP $_{\emptyset}$ (corroborating stability results in few-shot classification, cf. Tab. 2a), while Tip-adapter-F and TaskRes dramatically drop by **-2.09%** and **-10.21%**, resp.

Base-to-new generalization. In this setting, we divide all classes into two groups: base and new classes. Training is performed on base classes and testing on both base and new ones. The harmonic mean is reported to assess the trade-off. In Tab. 5, we see that ProLIP $_{\emptyset}$ significantly outperforms ProGrad [64] in *total harmonic mean* across 11 datasets. Additionally, ProLIP $_{\emptyset}$ is competitive with MaPLe [25], a method specifically designed for few-shot generalization. For comparison fairness, we report the three variants of MaPLe: MaPLe ‡ trains 9 \times more parameters than ProLIP (3.55M vs. 0.39M); MaPLe † trains a similar number of parameters (0.41M); MaPLe * is a shallow version that trains prompts only on the first layer of vision and language branches. Our method is architecture agnostic,

Method	RN50		RN101		ViT-B/16		ViT-B/32	
	IN	OOD	IN	OOD	IN	OOD	IN	OOD
CLIP (0-shot)	60.34	43.31	61.24	48.71	68.79	59.87	62.00	50.06
LP	41.29	21.19	47.01	28.33	54.70	35.09	46.77	28.81
CoOp	61.34	40.84	63.99	47.48	69.86	58.32	64.74	48.06
CoCoOp	61.04	40.42	63.59	47.34	70.13	58.17	64.63	47.93
Prograd	62.17	42.23	64.98	48.53	70.45	59.05	65.36	49.39
TaskRes	62.61	<u>42.55</u>	65.57	48.19	71.01	<u>59.59</u>	<u>65.99</u>	49.63
Tip-Adapter-F	60.88	41.72	64.85	<u>48.64</u>	70.17	59.04	65.63	49.97
ProLIP $_{\emptyset}$	<u>62.55</u>	43.20	<u>65.11</u>	48.81	<u>70.94</u>	59.97	66.00	<u>49.86</u>

Table 4. **Domain generalization.** 4-shot training on ImageNet (source) and evaluation on OOD variants (IN-V2, IV-S, IN-A, IN-R) with different visual backbones. We report accuracy over source ImageNet (IN) along with the average only over OOD variants to show generalization (‘OOD’). All baselines are reported from ProGrad [64] except for TaskRes and Tip-Adapter-F which we re-implemented.

	Base	New	H				
CLIP	61.72	65.91	63.75	CLIP	69.34	74.22	71.70
CoOp	71.96	61.26	66.18	CoOp	82.69	63.22	71.66
CoCoOp	72.23	60.77	66.01	CoCoOp	80.47	71.69	75.83
ProGrad	<u>73.29</u>	65.96	<u>69.43</u>	MaPLe*	80.10	73.52	76.67
ProLIP $_{\emptyset}$	75.45	69.43	72.31	MaPLe†	82.29	74.34	78.11
				MaPLe‡	82.28	75.14	<u>78.55</u>
				ProLIP $_{\emptyset}$	83.85	74.78	79.08

(a) ResNet-50

(b) ViT-B/16

Table 5. **Base-to-new.** Performance comparison of methods on ResNet-50 and ViT-B/16 architectures across 11 datasets.

while all versions of MaPLe work only on ViTs and require backpropagation over the entire vision and text encoders.

5.5. Analysis and Discussion

Comparison to full and last layer fine-tuning. We compare ProLIP $_{\emptyset}$ with full fine-tuning of the visual backbone. Results in Tab. 6 show that full fine-tuning is far behind ProLIP $_{\emptyset}$, and even degrades zero-shot performance for $N = 1, 2$ and 4-shots. LR is 10^{-5} for these experiments, and ProLIP $_{\emptyset}$ is shown for different λ values (including $\lambda = 0$). These results confirm that full fine-tuning faces a high risk of overfitting especially in low-shot regimes, advocating for PEFT methods like ProLIP.

Moreover, we show the results of fine-tuning the last layer (*i.e.*, the attention pooling layer) of the backbone. For the same LR = 10^{-5} , the performance lags behind ProLIP $_{\emptyset}$, with 8 \times more trainable parameters. Importantly, we also add results of last-layer fine-tuning when we increase LR to 10^{-4} , showing dramatically decreased performance, especially for extremely low-shot setting (*e.g.*, 1-shot).

Complementarity to other methods. Tab. 8 corroborates the complementarity of ProLIP with other methods, showing the benefit of combining ProLIP $_{\emptyset}$ with either TaskRes or Tip-Adapter-F. We argue, from the same perspective of logit bias discussed in [45], that each of these methods learns a specific bias on top of zero-shot CLIP, and

Method	# params	$N = 1$	2	4	8	16
CLIP (0-shot)	-				58.89	
Full Fine-tuning	38.32M	46.09	51.85	58.06	62.22	67.74
Last layer FT (10^{-5})	14.79M	61.26	64.37	67.99	71.58	75.53
Last layer FT (10^{-4})	14.79M	47.47	54.84	62.69	68.98	74.56
ProLIP $_{\emptyset}$ ($\lambda = 0$)	2.10M	62.84	66.35	69.69	72.89	75.65
ProLIP $_{\emptyset}$ ($\lambda = 1/N$)	2.10M	64.28	<u>67.07</u>	69.68	72.57	75.20
ProLIP $_{\emptyset}$ ($\lambda = 1/N^2$)	2.10M	64.28	67.32	70.22	73.10	75.68

Table 6. **Comparison to full fine-tuning.** We report the classification accuracy (%) averaged over 11 datasets, comparing ProLIP $_{\emptyset}$ to full fine-tuning of the vision encoder, and fine-tuning (‘FT’) only the last layer, *i.e.* the attention pooling layer.

that these biases contain orthogonal information. For instance, TaskRes learns an element-wise adapter on top of the text embeddings (*i.e.*, the classifier weights), while Tip-Adapter-F learns an adapter initialized with intra-modal similarities (*i.e.*, cache model). ProLIP’s learned bias stems from re-leveraging the pre-projection features to create new combinations adapted to the fixed probe. Interestingly, only a marginal improvement is observed when combining ProLIP and RLA, which suggests that they are best viewed as alternatives—an expected outcome since both methods learn linear transformations of visual features, leading to redundancies when combined together. More details are provided in the supplementary material.

ProLIP with other CLIP-like models. To verify the generalizability of ProLIP to other CLIP-like models, we provide in Tab. 7 average results across 11 datasets for ProLIP with SigLIP [56] ViT-B/16. Despite high zero-shot accuracy (+16.37% higher than zero-shot CLIP using RN50), ProLIP further advances the accuracy for all few-shot settings. In contrast with CLIP, which benefits from augmented views of the data, we surprisingly found that for SigLIP, adding more views does not improve the accuracy so we employed only one view. Subsequently, saving pre-projected features is extremely fast (a maximum of 57 sec. on a single V100-32GB GPU for 16-shot ImageNet), with training taking only around 7 sec. Moreover, in the validation-free setting, ProLIP $_{\emptyset}$ exhibits remarkable robustness to the learning rate (see standard deviation values in Tab. 7), which aligns with our previous results with CLIP (Tab. 2a).

We believe ProLIP can be further applied to other domains, like PointCLIPV2 [65] for 3D point cloud few-shot classification. ProLIP might relax the need for weight combination of the logits of multiple views, as this knowledge can be internalized in the projection weights by showing different views across iterations.

5.6. ProLIP for Test-time Adaptation

In this section, our goal is to show that ProLIP can be applied beyond supervised few-shot CLIP adaptation. Motivated by the risk of “overfitting” the source domain in clas-

Method	$N = 1$	2	4	8	16
SigLIP (0-shot)	75.26				
ProLIP (grid search)	78.28	80.49	82.29	84.10	85.82
ProLIP $_{\emptyset}$ ($\lambda = 1/N$)	77.45 ± 0.00	78.70 ± 0.00	80.06 ± 0.01	81.79 ± 0.04	83.55 ± 0.06
ProLIP $_{\emptyset}$ ($\lambda = 1/N^2$)	77.45 ± 0.00	79.38 ± 0.00	81.50 ± 0.01	83.68 ± 0.03	85.35 ± 0.03

Table 7. **ProLIP with SigLIP.** We report the classification accuracy (%) averaged over 11 datasets and 10 seeds for ProLIP and ProLIP $_{\emptyset}$ with SigLIP ViT-B/16 [56]. For ProLIP $_{\emptyset}$, we report average and standard deviation over 3 LR $\in\{10^{-4}, 10^{-3}, 10^{-2}\}$.

Method	$N = 1$	2	4	8	16
CLIP (0-shot)	58.89				
ProLIP $_{\emptyset}$	64.40	67.28	70.08	72.97	75.57
ProLIP $_{\emptyset}$ + RLA	64.47	67.38	70.19	73.02	75.65
ProLIP $_{\emptyset}$ + Tip-Adapter-F [58]	64.53	67.47	70.30	73.23	75.89
ProLIP $_{\emptyset}$ + TaskRes [53]	65.01	68.18	71.00	73.78	76.23

Table 8. **Complementarity to other methods.** We report the classification accuracy (%) averaged over 11 datasets and 10 seeds. LR is fixed to 10^{-4} for all datasets, and $\lambda = 1/N$.

Method	IN	IN-A	IN-V2	IN-R	IN-S	Average	Avg. OOD
CLIP (0-shot)	60.33	23.79	53.31	60.58	35.46	46.69	43.29
<i>w/o few-shot training on IN</i>							
TPT [40]	<u>60.74</u>	<u>26.67</u>	<u>54.70</u>	<u>59.11</u>	<u>35.09</u>	47.26	43.89
ProLIP _{test-time}	62.00	33.76	56.03	62.69	37.29	50.35	47.44
<i>w/ 16-shot training on IN</i>							
CoOp [40]	63.33	23.06	55.40	56.60	34.67	46.61	42.43
TPT + CoOp [40]	64.73	30.32	57.83	58.99	35.86	49.55	45.75
ProLIP	64.48	22.75	56.24	<u>59.56</u>	34.80	47.57	43.34
ProLIP _{test-time} + ProLIP	66.90	32.96	58.77	61.78	36.97	51.48	47.62

Table 9. **Robustness to natural distribution shifts in test-time adaptation.** Experiments are done with RN50 backbone, without few-shot training on IN (top) and with 16-shot training (bottom).

sic prompt tuning methods [62, 63], Shu *et al.* [40] pioneered test-time prompt tuning (TPT), aiming to learn adaptive prompts on the fly using a single test image.

TPT background knowledge. TPT aims to learn a context specific to each test image in an unsupervised way. Given an unlabeled test image \mathbf{I}_{test} , the prompt is learned by minimizing the average prediction entropy over different augmented views of \mathbf{I}_{test} . Moreover, *confidence selection* filters out the augmented views with high entropy predictions, which might lack important information for classification. More details are provided in the supplementary material.

Test-time ProLIP. We do not introduce a new way for CLIP test-time adaptation but simply follow the same experimental setting as TPT (*i.e.*, 1-step entropy minimization of averaged prediction probability distribution, confidence selection), although ProLIP optimizes the projection weight matrix \mathbf{W}_o instead of the prompt as in TPT. We name this ProLIP variant as ProLIP_{test-time}. Tab. 9 shows that ProLIP_{test-time} yields superior results to TPT on ImageNet and natural distribution shifts, while being one order

of magnitude faster to train. For direct comparison, we separate methods that perform 16-shot training on ImageNet. Of note, even without few-shot training, ProLIP_{test-time} still outperforms CoOp and TPT+CoOp. We further advance ProLIP_{test-time} results with 16-shot training.

6. Conclusion

We propose a simple and efficient method for adapting CLIP to few-shot classification by fine-tuning the visual projection matrix. Moreover, we show advantages of including a Frobenius norm regularizer: it prevents the drift from pretrained weights and improves robustness to hyper-parameter choice, thus making our method an appealing approach to practical few-shot adaptation. Additionally, we reflect on the practice of using non-linear adapters from our method’s perspective and propose a strong and robust regularized linear adapter. We provide evidence of the competitiveness of ProLIP in few-shot classification, generalization and test-time adaptation, as well as its complementarity with other methods, rendering it a potential general framework for further applications.

Acknowledgment. This work was partially funded by French project SIGHT (ANR-20-CE23-0016). It was performed using HPC resources from GENCI-IDRIS (Grants AD011014477R1, AD011012808R3). The authors thank Clément Weinreich for insightful discussion.

References

- Peter L Bartlett and Shahar Mendelson. Rademacher and gaussian complexities: Risk bounds and structural results. *JMLR*, 3(Nov):463–482, 2002. 3
- Christopher M Bishop and Nasser M Nasrabadi. *Pattern recognition and machine learning*. Springer, 2006. 2
- Lukas Bossard, Matthieu Guillaumin, and Luc Van Gool. Food-101-mining discriminative components with random forests. In *ECCV*, 2014. 5
- Tom Brown, Benjamin Mann, Nick Ryder, Melanie Subbiah, Jared D Kaplan, Prafulla Dhariwal, Arvind Neelakantan, Pranav Shyam, Girish Sastry, Amanda Askell, et al. Language models are few-shot learners. In *NeurIPS*, 2020. 3
- Mathilde Caron, Hugo Touvron, Ishan Misra, Hervé Jégou, Julien Mairal, Piotr Bojanowski, and Armand Joulin. Emerging properties in self-supervised vision transformers. In *ICCV*, 2021. 3
- Guangyi Chen, Weiran Yao, Xiangchen Song, Xinyue Li, Yongming Rao, and Kun Zhang. PLOT: Prompt learning with optimal transport for vision-language models. In *ICLR*, 2023. 1, 2, 5, 6, 19, 20
- Xinlei Chen, Saining Xie, and Kaiming He. An empirical study of training self-supervised vision transformers. In *ICCV*, 2021. 3
- Mircea Cimpoi, Subhransu Maji, Iasonas Kokkinos, Sammy Mohamed, and Andrea Vedaldi. Describing textures in the wild. In *CVPR*, 2014. 4

[9] Jia Deng, Wei Dong, Richard Socher, Li-Jia Li, Kai Li, and Li Fei-Fei. Imagenet: A large-scale hierarchical image database. In *CVPR*, 2009. 4

[10] Alexey Dosovitskiy, Lucas Beyer, Alexander Kolesnikov, Dirk Weissenborn, Xiaohua Zhai, Thomas Unterthiner, Mostafa Dehghani, Matthias Minderer, Georg Heigold, Sylvain Gelly, Jakob Uszkoreit, and Neil Houlsby. An image is worth 16x16 words: Transformers for image recognition at scale. In *ICLR*, 2021. 19

[11] Matteo Farina, Massimiliano Mancini, Giovanni Iacca, and Elisa Ricci. Rethinking few-shot adaptation of vision-language models in two stages. In *CVPR*, 2025. 3, 15

[12] Li Fei-Fei, Rob Fergus, and Pietro Perona. Learning generative visual models from few training examples: An incremental bayesian approach tested on 101 object categories. In *CVPR Workshops*, 2004. 4

[13] Peng Gao, Shijie Geng, Renrui Zhang, Teli Ma, Rongyao Fang, Yongfeng Zhang, Hongsheng Li, and Yu Qiao. Clip-adapter: Better vision-language models with feature adapters. *IJCV*, 2024. 1, 2, 4, 5, 17, 19, 20

[14] Muhammad Waleed Gondal, Jochen Gast, Inigo Alonso Ruiz, Richard Droste, Tommaso Macri, Suren Kumar, and Luitpold Staudigl. Domain aligned clip for few-shot classification. In *WACV*, 2024. 2

[15] Henry Gouk, Timothy Hospedales, and Massimiliano Pontil. Distance-based regularisation of deep networks for fine-tuning. In *ICLR*, 2021. 3

[16] Trevor Hastie, Robert Tibshirani, Jerome H Friedman, and Jerome H Friedman. *The elements of statistical learning: data mining, inference, and prediction*. Taylor & Francis, 2009. 3

[17] Kaiming He, Xiangyu Zhang, Shaoqing Ren, and Jian Sun. Deep residual learning for image recognition. In *CVPR*, 2016. 19

[18] Patrick Helber, Benjamin Bischke, Andreas Dengel, and Damian Borth. Eurosat: A novel dataset and deep learning benchmark for land use and land cover classification. *IEEE Journal of Selected Topics in Applied Earth Observations and Remote Sensing*, 2019. 1, 5

[19] Dan Hendrycks, Steven Basart, Norman Mu, Saurav Kadavath, Frank Wang, Evan Dorundo, Rahul Desai, Tyler Zhu, Samyak Parajuli, Mike Guo, et al. The many faces of robustness: A critical analysis of out-of-distribution generalization. In *ICCV*, 2021. 5

[20] Dan Hendrycks, Kevin Zhao, Steven Basart, Jacob Steinhardt, and Dawn Song. Natural adversarial examples. In *CVPR*, 2021. 5

[21] Neil Houlsby, Andrei Giurgiu, Stanislaw Jastrzebski, Bruna Morrone, Quentin De Laroussilhe, Andrea Gesmundo, Mona Attariyan, and Sylvain Gelly. Parameter-efficient transfer learning for nlp. In *ICML*, 2019. 2

[22] Edward J Hu, Yelong Shen, Phillip Wallis, Zeyuan Allen-Zhu, Yuanzhi Li, Shean Wang, Lu Wang, and Weizhu Chen. Lora: Low-rank adaptation of large language models. In *ICLR*, 2022. 2, 15

[23] Yunshi Huang, Fereshteh Shakeri, Jose Dolz, Malik Boudiaf, Houda Bahig, and Ismail Ben Ayed. LP++: A surprisingly strong linear probe for few-shot clip. In *CVPR*, 2024. 1, 2, 3, 5, 17, 18, 19, 20

[24] Menglin Jia, Luming Tang, Bor-Chun Chen, Claire Cardie, Serge Belongie, Bharath Hariharan, and Ser-Nam Lim. Visual prompt tuning. In *ECCV*, 2022. 2

[25] Muhammad Uzair Khattak, Hanoona Rasheed, Muhammad Maaz, Salman Khan, and Fahad Shahbaz Khan. Maple: Multi-modal prompt learning. In *CVPR*, 2023. 1, 2, 3, 4, 5, 7, 13

[26] Muhammad Uzair Khattak, Syed Talal Wasim, Muzammal Naseer, Salman Khan, Ming-Hsuan Yang, and Fahad Shahbaz Khan. Self-regulating prompts: Foundational model adaptation without forgetting. In *ICCV*, 2023. 2

[27] James Kirkpatrick, Razvan Pascanu, Neil Rabinowitz, Joel Veness, Guillaume Desjardins, Andrei A Rusu, Kieran Milan, John Quan, Tiago Ramalho, Agnieszka Grabska-Barwinska, et al. Overcoming catastrophic forgetting in neural networks. *Proceedings of the national academy of sciences*, 2017. 3

[28] Jonathan Krause, Michael Stark, Jia Deng, and Li Fei-Fei. 3d object representations for fine-grained categorization. In *ICCV Workshops*, 2013. 5

[29] Ananya Kumar, Aditi Raghunathan, Robbie Jones, Tengyu Ma, and Percy Liang. Fine-tuning can distort pretrained features and underperform out-of-distribution. In *ICLR*, 2022. 1, 2

[30] Xiang Lisa Li and Percy Liang. Prefix-tuning: Optimizing continuous prompts for generation. *ACL*, 2021. 2

[31] Zhiqiu Lin, Samuel Yu, Zhiyi Kuang, Deepak Pathak, and Deva Ramanan. Multimodality helps unimodality: Cross-modal few-shot learning with multimodal models. In *CVPR*, 2023. 1, 2, 6, 17

[32] Subhransu Maji, Esa Rahtu, Juho Kannala, Matthew Blaschko, and Andrea Vedaldi. Fine-grained visual classification of aircraft. *arXiv*, 2013. 1, 5

[33] Maria-Elena Nilsback and Andrew Zisserman. Automated flower classification over a large number of classes. In *ICVGIP*, 2008. 5

[34] Omkar M Parkhi, Andrea Vedaldi, Andrew Zisserman, and CV Jawahar. Cats and dogs. In *CVPR*, 2012. 5

[35] Adam Paszke, Sam Gross, Francisco Massa, Adam Lerer, James Bradbury, Gregory Chanan, Trevor Killeen, Zeming Lin, Natalia Gimelshein, Luca Antiga, et al. Pytorch: An imperative style, high-performance deep learning library. In *NeurIPS*, 2019. 3

[36] Alec Radford, Jong Wook Kim, Chris Hallacy, Aditya Ramesh, Gabriel Goh, Sandhini Agarwal, Girish Sastry, Amanda Askell, Pamela Mishkin, Jack Clark, et al. Learning transferable visual models from natural language supervision. In *ICML*, 2021. 1, 2, 5, 19, 20

[37] Aditya Ramesh, Mikhail Pavlov, Gabriel Goh, Scott Gray, Chelsea Voss, Alec Radford, Mark Chen, and Ilya Sutskever. Zero-shot text-to-image generation. In *ICML*, 2021. 3

[38] Benjamin Recht, Rebecca Roelofs, Ludwig Schmidt, and Vaishaal Shankar. Do imagenet classifiers generalize to imagenet? In *ICML*, 2019. 5

[39] Andreas Rücklé, Gregor Geigle, Max Glockner, Tilman Beck, Jonas Pfeiffer, Nils Reimers, and Iryna Gurevych. Adapterdrop: On the efficiency of adapters in transformers. In *EMNLP*, 2021. 2

[40] Manli Shu, Weili Nie, De-An Huang, Zhiding Yu, Tom Goldstein, Anima Anandkumar, and Chaowei Xiao. Test-time prompt tuning for zero-shot generalization in vision-language models. In *NeurIPS*, 2022. 5, 9, 13

[41] Yang Shu, Xingzhuo Guo, Jialong Wu, Ximei Wang, Jianmin Wang, and Mingsheng Long. Clipood: Generalizing clip to out-of-distributions. In *ICML*, 2023. 2

[42] Julio Silva-Rodriguez, Sina Hajimiri, Ismail Ben Ayed, and Jose Dolz. A closer look at the few-shot adaptation of large vision-language models. In *CVPR*, 2024. 1, 2, 3, 5, 6, 7

[43] Lin Song, Ruoyi Xue, Hang Wang, Hongbin Sun, Yixiao Ge, Ying Shan, et al. Meta-adapter: An online few-shot learner for vision-language model. In *NeurIPS*, 2023. 1, 2

[44] K Soomro. Ucf101: A dataset of 101 human actions classes from videos in the wild. *arXiv*, 2012. 4

[45] Yuwei Tang, Zhenyi Lin, Qilong Wang, Pengfei Zhu, and Qinghua Hu. Amu-tuning: Effective logit bias for clip-based few-shot learning. In *CVPR*, 2024. 3, 8, 15

[46] Ashish Vaswani, Noam Shazeer, Niki Parmar, Jakob Uszkoreit, Llion Jones, Aidan N Gomez, Łukasz Kaiser, and Illia Polosukhin. Attention is all you need. In *NeurIPS*, 2017. 19

[47] Dequan Wang, Evan Shelhamer, Shaoteng Liu, Bruno Olshausen, and Trevor Darrell. Tent: Fully test-time adaptation by entropy minimization. In *ICLR*, 2021. 7, 15

[48] Haohan Wang, Songwei Ge, Zachary Lipton, and Eric P Xing. Learning robust global representations by penalizing local predictive power. In *NeurIPS*, 2019. 5

[49] Zhengbo Wang, Jian Liang, Lijun Sheng, Ran He, Zilei Wang, and Tieniu Tan. A hard-to-beat baseline for training-free CLIP-based adaptation. In *ICLR*, 2024. 2

[50] Zhixiang Wei, Lin Chen, Yi Jin, Xiaoxiao Ma, Tianle Liu, Pengyang Ling, Ben Wang, Huaian Chen, and Jinjin Zheng. Stronger fewer & superior: Harnessing vision foundation models for domain generalized semantic segmentation. In *CVPR*, 2024. 2

[51] Jianxiong Xiao, James Hays, Krista A Ehinger, Aude Oliva, and Antonio Torralba. Sun database: Large-scale scene recognition from abbey to zoo. In *CVPR*, 2010. 4

[52] Hantao Yao, Rui Zhang, and Changsheng Xu. Visual-language prompt tuning with knowledge-guided context optimization. In *CVPR*, 2023. 5, 19, 20

[53] Tao Yu, Zhihe Lu, Xin Jin, Zhibo Chen, and Xinchao Wang. Task residual for tuning vision-language models. In *CVPR*, 2023. 1, 2, 3, 4, 5, 6, 9

[54] Elad Ben Zaken, Shauli Ravfogel, and Yoav Goldberg. Bitfit: Simple parameter-efficient fine-tuning for transformer-based masked language-models. In *ACL*, 2022. 2

[55] Maxime Zanella and Ismail Ben Ayed. Low-rank few-shot adaptation of vision-language models. In *CVPR Workshops*, 2024. 2, 4, 7, 15

[56] Xiaohua Zhai, Basil Mustafa, Alexander Kolesnikov, and Lucas Beyer. Sigmoid loss for language image pre-training. In *ICCV*, 2023. 2, 8, 9

[57] Jeffrey O Zhang, Alexander Sax, Amir Zamir, Leonidas Guibas, and Jitendra Malik. Side-tuning: a baseline for network adaptation via additive side networks. In *ECCV*, 2020. 2

[58] Renrui Zhang, Wei Zhang, Rongyao Fang, Peng Gao, Kun-chang Li, Jifeng Dai, Yu Qiao, and Hongsheng Li. Tip-adapter: Training-free adaption of clip for few-shot classification. In *ECCV*, 2022. 1, 2, 3, 4, 5, 6, 9, 17, 18, 19, 20

[59] Renrui Zhang, Xiangfei Hu, Bohao Li, Siyuan Huang, Han-qiue Deng, Yu Qiao, Peng Gao, and Hongsheng Li. Prompt, generate, then cache: Cascade of foundation models makes strong few-shot learners. In *CVPR*, 2023. 3

[60] Bingchen Zhao, Haoqin Tu, Chen Wei, Jieru Mei, and Ci-hang Xie. Tuning layernorm in attention: Towards efficient multi-modal LLM finetuning. In *ICLR*, 2024. 7, 15

[61] Zexuan Zhong, Dan Friedman, and Danqi Chen. Factual probing is [mask]: Learning vs. learning to recall. *ACL*, 2021. 2

[62] Kaiyang Zhou, Jingkang Yang, Chen Change Loy, and Ziwei Liu. Conditional prompt learning for vision-language models. In *CVPR*, 2022. 1, 2, 5, 7, 9

[63] Kaiyang Zhou, Jingkang Yang, Chen Change Loy, and Ziwei Liu. Learning to prompt for vision-language models. *IJCV*, 2022. 1, 2, 5, 9, 19, 20

[64] Beier Zhu, Yulei Niu, Yucheng Han, Yue Wu, and Hanwang Zhang. Prompt-aligned gradient for prompt tuning. In *ICCV*, 2023. 1, 2, 5, 6, 7, 8, 13, 19, 20

[65] Xiangyang Zhu, Renrui Zhang, Bowei He, Ziyu Guo, Ziyao Zeng, Zipeng Qin, Shanghang Zhang, and Peng Gao. Point-clip v2: Prompting clip and gpt for powerful 3d open-world learning. In *ICCV*, 2023. 8

[66] Xiangyang Zhu, Renrui Zhang, Bowei He, Aojun Zhou, Dong Wang, Bin Zhao, and Peng Gao. Not all features matter: Enhancing few-shot clip with adaptive prior refinement. In *ICCV*, 2023. 3

CLIP's Visual Embedding Projector is a Few-shot Cornucopia

Supplementary Material

Algorithm 1 PyTorch-like pseudo-code for ProLIP.

```

# target: Ground truth
# lmdu: regularization loss weight
# Wo : Pretrained projection matrix
# bo : Pretrained bias term (only ResNet, 0 for ViT)
# xo: output visual embeddings (N*K, Do)
# text_weights: normalized embeddings of classnames (K,D)

# Copy initial weights for use in the regularization loss
Wo_0 = copy.deepcopy(Wo)
# Set embedding projection matrix as trainable weights
Wo.requires_grad = True
bo.requires_grad = False

v = xo @ Wo + bo
v = 12_normalize(v, dim=-1)

#compute the cosine similarity scores
logits = 100. * v @ text_weights.T

#compute regularized loss
SE_loss = nn.MSELoss(reduction='sum')
loss = CE_loss(logits, target) + lmdu * SE_loss(Wo, Wo_0)

```

This document provides:

- A PyTorch-like pseudo-code for ProLIP, shown in Algorithm 1.
- Per-dataset performance of few-shot classification with few-shot validation in Sec. 7, complementing Tab. 1.
- Grid search and hyperparameter sensitivity in Sec. 8, as well as the data of Tab. 2a, Tab. 2b and Fig. 4.
- Base-to-new generalization detailed performance in Sec. 9.
- Experiments on fine-tuning the text embedding projection matrix in Sec. 10.
- Test-time adaptation details in Sec. 11.
- Additional comparison of ProLIP_θ to architecture-specific methods in Sec. 12.
- Details about RLA, complementarity analysis, and additional experiments and ablations in Sec. 13.
- Training of ProLIP in Sec. 14.
- Preliminaries on CLIP in Sec. 15.

7. Details on few-shot classification with few-shot validation

In addition to the average across datasets in Tab. 1, Tabs. 23–24 provide the *per-dataset performance* of all methods, with for each the average accuracy over 10 seeds (*i.e.*, support sets). ProLIP performs particularly well on DTD, UCF101, StanfordCars, FGVCAircraft and EuroSAT. For some specific settings, *e.g.*, 1-shot DTD, 16-shot StanfordCars, 8 and 16-shot FGVCAircraft, the improvements over state-of-the-art are significant. On the other hand, for datasets like Ox-

fordPets and Food101, where the zero-shot performance is already good, ProLIP and other baselines are outperformed by prompt learning methods (*e.g.*, ProGrad). This might be due to the relatively lower number of parameters in the latter, making them less prone to overfitting in very low-shot settings; when the number of shots increases, *e.g.*, 8–16 shots, ProLIP and prompt learning perform on par.

Future research may include the zero-shot accuracy on the few-shot training set in the parametric formulation of the regularization loss weight (*i.e.*, λ). That is, the higher the zero-shot accuracy, the smaller should be the distance between the fine-tuned projection matrix and the pretrained one (*i.e.*, higher λ).

8. ProLIP hyperparameters study

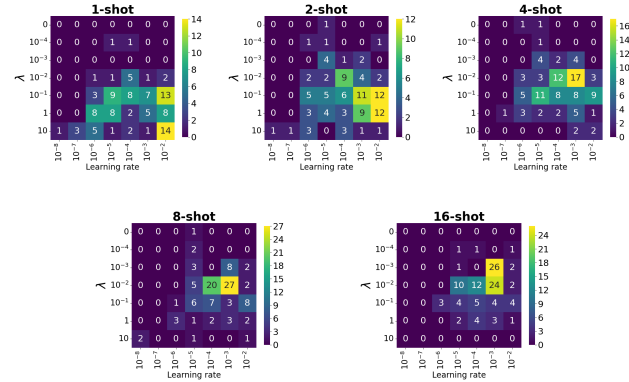


Figure 6. **Hyperparameters selected by grid search.** Learning rates and regularization loss weights λ found with grid search on the few-shot validation set. The distribution of these hyperparameters are shown for each few-shot setting ($N = 1, 2, 4, 8, 16$).

Grid search. Fig. 6 shows the distribution of hyperparameters found by grid search on the few-shot validation set (cf. Tab. 1). We draw two observations:

1. The learning rates span a wide range of values, and high values like 10^{-3} and 10^{-2} are selected several times, which would cause severe overfitting when no regularization is used (cf. Tab. 11 and Fig. 4).
2. $\lambda = 0$ is rarely selected, meaning that based on the few-shot validation set, regularized projection matrices generalize better.

Hyperparameter sensitivity. Tab. 10 complements Fig. 4, where ProLIP is trained for different fixed learning

rates, with fixed regularization loss weight λ . Looking at the values, we make the following observations:

1. For low learning rates (*i.e.*, $10^{-5}, 10^{-6}$), unregularized ProLIP shows good performance for different values of N , demonstrating the effectiveness of simply fine-tuning the visual projection matrix. However, the performance drops significantly when the LR increases.
2. A higher value of λ works better for fewer training shots N , and vice versa. This effect is increasingly visible when the LR increases. Such observation is expected: with less data we need more regularization as overfitting risk is higher, and this is the base for formulating λ as a decreasing function of N (See Tab. 11, which shows the detailed numerical results of Tab. 2a).

9. Details on base-to-new generalization

Metrics details. Previous works [25, 64] calculate the *total harmonic mean* over datasets in two different ways.

To extend Tab. 5, in Tab. 12 we report for each architecture both ways of calculating the *total harmonic means*, renaming them H_{t1} and H_{t2} for disambiguation. It highlights the superiority of our method, regardless of the total harmonic mean used. We also detail the computation below.

In ProGrad [64], the total harmonic mean over the 11 datasets is computed as *the average harmonic means of individual datasets*. This writes:

$$H_{t1} = \frac{1}{11} \sum_{i=1}^{11} \text{HM}_i, \quad (9)$$

$\text{HM}_i = 2 \times \frac{\text{acc}_{b_i} \times \text{acc}_{n_i}}{\text{acc}_{b_i} + \text{acc}_{n_i}}$ being the harmonic mean of dataset i . Here, acc_{b_i} and acc_{n_i} denote the accuracy on base and new classes for dataset i , respectively.

Instead in MaPLe [25], the total harmonic mean over the 11 datasets is calculated as *the harmonic mean of average base and average new classes accuracies*:

$$H_{t2} = 2 \times \frac{\text{acc}_b \times \text{acc}_n}{\text{acc}_b + \text{acc}_n}, \quad (10)$$

where $\text{acc}_b = \frac{1}{11} \sum_{i=1}^{11} \text{acc}_{b_i}$ and $\text{acc}_n = \frac{1}{11} \sum_{i=1}^{11} \text{acc}_{n_i}$.

Per-dataset performance. We report in Tab. 17 and Tab. 18 the per-dataset accuracy for base and new classes, as well as the harmonic mean metrics.

10. Fine-tuning the text embedding projector

Can the text embedding projector work? As discussed in Sec. 3, CLIP also maps text embeddings to the shared space using a projection matrix. Here, instead of fine-tuning the visual projection matrix \mathbf{W}_o , we fine-tune its textual counterpart \mathbf{W}_{ot} , with the same strategy adopted in

ProLIP $_{\emptyset}$. That is, the visual backbone, including \mathbf{W}_o , is frozen. Only \mathbf{W}_{ot} is trained with:

$$L_{\text{ProLIP}(\text{text})} = L(\mathbf{W}_{ot}) + \lambda \|\mathbf{W}_{ot} - \mathbf{W}_{ot}^{(0)}\|_F^2, \quad (11)$$

where λ is set to $\frac{1}{N}$. Tab. 13 shows that this variant is also a strong baseline, though underperforming ProLIP $_{\emptyset}$ where the visual embedding projection is fine-tuned. This experiment gives a positive signal on the extendability of our method to other modalities.

Tab. 14 complements Tab. 13, showing the performance of this version, coined ‘ProLIP $_{\emptyset}$ (text)’, for different values of LR. We note that this baseline is strong, yet still underperforming ProLIP $_{\emptyset}$ and exhibiting more sensitivity to the choice of LR.

11. Details on test-time ProLIP

TPT [40] learns a single prompt for each test image using an unsupervised loss function. Given a test image \mathbf{I}_{test} , the image is augmented N_{views} times using a family of random augmentations \mathcal{A} . Predictions are made for each view, and the training consists of minimizing the entropy of the averaged probability distribution of these predictions:

$$\mathbf{p}^* = \operatorname{argmin}_{\mathbf{p}} - \sum_{i=1}^K \tilde{p}_{\mathbf{p}}(y_i | \mathbf{I}_{\text{test}}) \log \tilde{p}_{\mathbf{p}}(y_i | \mathbf{I}_{\text{test}}), \quad (12)$$

where

$$\tilde{p}_{\mathbf{p}}(y_i | \mathbf{I}_{\text{test}}) = \frac{1}{N_{\text{views}}} \sum_{i=1}^{N_{\text{views}}} p_{\mathbf{p}}(y_i | \mathcal{A}_i(\mathbf{I}_{\text{test}})). \quad (13)$$

In addition, *confidence selection* is used to filter out predictions with high entropy, which are considered as noisy. Self-entropy is computed for each of the N_{views} ; a fixed cutoff percentile ρ keeps only predictions with lower entropy than τ . In Equation 12, $\tilde{p}_{\mathbf{p}}$ becomes:

$$\tilde{p}_{\mathbf{p}}(y | \mathbf{I}_{\text{test}}) = \frac{1}{\rho N} \sum_{i=1}^{N_{\text{views}}} \mathbb{1}_{\{H(p_i) \leq \tau\}} p_{\mathbf{p}}(y | \mathcal{A}_i(\mathbf{I}_{\text{test}})). \quad (14)$$

We apply the same framework (*i.e.*, loss function, confidence selection) with the only difference of minimizing Equation 12 over \mathbf{W}_o instead of the prompt \mathbf{p} . For a fair comparison, we use the same number of steps for training (*i.e.*, 1 step) and the same value of the cutoff percentile $\rho = 0.1$. The learning rate is 10^{-4} . Note that, measured on ImageNet, ProLIP is ~ 13 times faster than TPT, as the latter requires backpropagation through the whole text encoder, while in our case backpropagation is limited to the visual projection layer and is not applied on the text encoder. We also stress that since we perform only 1 step of training, the regularization loss cannot be used as the first value it takes is 0 (initially the fine-tuned projection matrix is equal to the pre-trained one).

Method	$N = 1$	2	4	8	16
CLIP (0-shot)	58.89				
ProLIP (grid search)	64.21	67.43	70.58	73.73	76.50
ProLIP, $LR=10^{-6}$	$\lambda = 1$	62.85	64.98	66.66	68.13
	$\lambda = 10^{-1}$	63.69	66.51	68.87	71.07
	$\lambda = 10^{-2}$	63.73	66.62	69.09	71.42
	$\lambda = 0$	63.73	66.64	69.12	71.46
ProLIP, $LR=10^{-5}$	$\lambda = 1$	64.28	66.59	68.30	69.67
	$\lambda = 10^{-1}$	64.60	<u>67.49</u>	70.13	72.71
	$\lambda = 10^{-2}$	63.54	66.87	70.03	73.06
	$\lambda = 0$	62.84	66.35	69.69	72.89
ProLIP, $LR=10^{-4}$	$\lambda = 1$	64.40	66.86	68.82	70.37
	$\lambda = 10^{-1}$	<u>64.48</u>	67.51	<u>70.37</u>	73.08
	$\lambda = 10^{-2}$	60.45	64.73	69.04	72.85
	$\lambda = 0$	50.55	58.69	65.18	69.93
ProLIP, $LR=10^{-3}$	$\lambda = 1$	64.39	66.82	68.78	70.42
	$\lambda = 10^{-1}$	64.08	67.32	70.28	<u>73.17</u>
	$\lambda = 10^{-2}$	58.42	64.43	69.16	<u>72.94</u>
	$\lambda = 0$	40.05	49.60	56.35	60.33
ProLIP, $LR=10^{-2}$	$\lambda = 1$	64.25	66.83	68.75	70.36
	$\lambda = 10^{-1}$	63.04	67.03	70.05	72.75
	$\lambda = 10^{-2}$	53.58	61.43	67.47	71.92
	$\lambda = 0$	19.98	24.12	28.03	32.42

Table 10. **ProLIP sensitivity to hyperparameter choice.** Accuracy of ProLIP to the hyperparameters (learning rate LR and regularization weight λ) for $N \in \{1, 2, 4, 8, 16\}$ -shot settings. Each number is an average over 11 datasets, 10 seeds for each.

Method	$N = 1$	2	4	8	16
CLIP (0-shot)	58.89				
ProLIP $_{\emptyset}$, $\lambda = 1/N$	LR= 10^{-5}	64.28	67.07	69.68	72.57
	LR= 10^{-4}	64.40	67.28	70.08	72.97
	LR= 10^{-3}	64.39	67.20	70.01	73.02
	LR= 10^{-2}	64.25	67.20	69.98	72.70
	Average	64.33	<u>67.19</u>	<u>69.94</u>	<u>72.82</u>
ProLIP $_{\emptyset}$, $\lambda = 1/N^2$	LR= 10^{-5}	64.28	67.32	70.22	73.10
	LR= 10^{-4}	64.40	67.53	70.36	73.08
	LR= 10^{-3}	64.39	67.40	70.25	73.10
	LR= 10^{-2}	64.25	67.31	70.02	72.50
	Average	64.33	67.39	70.21	72.95
ProLIP $_{\emptyset}$, $\lambda = 0$	LR= 10^{-5}	62.84	66.35	69.69	72.89
	LR= 10^{-4}	50.55	58.69	65.18	69.93
	LR= 10^{-3}	40.05	49.60	56.35	60.33
	LR= 10^{-2}	19.98	24.12	28.03	32.42
	Average	43.36	49.69	54.81	58.89

Table 11. **ProLIP $_{\emptyset}$ with a parametric λ .** Accuracy (%) of ProLIP $_{\emptyset}$ with fixed learning rate (LR) and λ as a function of N . For each λ value, we report performance for different LRs and averaged across LRs. Numbers are averages over 11 datasets and 10 seeds. We highlight **best** and 2nd best for averages across LRs.

	Base	New	H_{t1}	H_{t2}		Base	New	H_{t1}	H_{t2}	
CLIP	61.72	65.91	63.64	63.75		CLIP	69.34	74.22	71.59	71.70
CoOp	71.96	61.26	65.58	66.18		CoOp	82.69	63.22	70.83	71.66
CoCoOp	72.23	60.77	65.35	66.01		CoCoOp	80.47	71.69	75.44	75.83
ProGrad	73.29	65.96	69.06	69.43		MaPLe	82.28	75.14	78.27	78.55
ProLIP $_{\emptyset}$	75.45	69.43	72.12	72.31		ProLIP $_{\emptyset}$	83.85	74.78	78.85	79.06

(a) ResNet-50

(b) ViT-B/16

Table 12. **Base-to-new.** Performance comparison of methods on ResNet-50 and ViT-B/16 architectures across 11 datasets with either H_{t1} (equation 9) or H_{t2} (equation 10). Numbers highlight the superiority of our method.

Method	$N = 1$	2	4	8	16
CLIP (0-shot)				58.89	
ProLIP $_{\emptyset}$ (text)	64.05	66.93	69.71	72.56	75.01
ProLIP $_{\emptyset}$ (ours)	64.33	67.19	69.94	72.82	75.46

Table 13. **Comparison to fine-tuning the text embedding projection matrix.** We report the classification accuracy (%) averaged over 11 datasets, 10 seeds, and 4 learning rates $LR \in \{10^{-5}, 10^{-4}, 10^{-3}, 10^{-2}\}$ where we fine-tune the text projection matrix instead of the visual one, with the same regularization strategy. We call this variant ‘ProLIP $_{\emptyset}$ (text)’ and use $\lambda = 1/N$.

Method	LR	$N = 1$	2	4	8	16
CLIP (0-shot)				58.89		
	10^{-5}	64.25	67.10	69.91	72.82	75.34
ProLIP $_{\emptyset}$ (text)	10^{-4}	64.13	67.14	70.01	72.80	75.20
	10^{-3}	63.99	66.74	69.52	72.41	75.00
	10^{-2}	63.81	66.72	69.39	72.21	74.51

Table 14. **Fine-tuning the text embedding projection matrix.** We report classification accuracy (%) of ‘ProLIP $_{\emptyset}$ (text)’ averaged over 11 datasets and 10 seeds, using different learning rates (LR).

Method	Cls.	B2N	Arch. Agnostic
CLIP-LoRA [55]	77.74	77.28	✗
ProLIP $_{\emptyset}$	76.26	79.06	✓

Table 15. **CLIP-LoRA vs. ProLIP $_{\emptyset}$.** Few-shot classification (‘Cls.’) accuracies are averages of 550 runs (11 datasets, 10 seeds, 5 few-shot settings), Base-to-new (‘B2N’) harmonic means are averages of 110 runs (11 datasets, 10 seeds, $N=16$ -shot setting). For fair comparison, we adopt ‘a photo of a {}.’ as template, similarly to CLIP-LoRA.

12. Comparison to architecture-specific baselines

Comparison to low-rank adaptation (LoRA). Zanella *et al.* [55] recently showed that applying low-rank adaptation (LoRA) [22] to CLIP is a competitive baseline to adapters and prompt learning. They apply LoRA on query, key and value matrices of the ViT, and show strong performance on the few-shot classification setting. We compare ProLIP $_{\emptyset}$

Arch.	Method	Cls.	Params
RN50	BatchNorm [47]	71.66	0.05M
	ProLIP $_{\emptyset}$	75.46	2.10M
ViT-B/16	LayerNorm [60]	78.13	0.07M
	ProLIP $_{\emptyset}$	81.00	0.39M

Table 16. **Normalization parameters tuning vs. ProLIP $_{\emptyset}$.** Few-shot classification (‘Cls.’) accuracies are averages of 110 runs (11 datasets & 10 seeds). The number of samples per class is $N = 16$.

to CLIP-LoRA [55] for ViT-B/16 on few-shot classification and base-to-new generalization. Few-shot classification results are averaged across 5 settings (*i.e.*, $N=\{1,2,4,8,16\}$), 11 datasets and 10 seeds, while base-to-new generalization results are averaged across 11 datasets and 10 seeds for $N = 16$. For a fair comparison, we use the template ‘a photo of a {}’ for the class names, similarly to CLIP-LoRA. The results are shown in Tab. 15. Slower than ProLIP, CLIP-LoRA works well on classification [55] but compromises base-to-new generalization (B2N) [11] and is specific to ViT.

Comparison to normalization techniques. We compare here ProLIP $_{\emptyset}$ to methods that fine-tune only affine normalization parameters for BatchNorm [47] in CNN and LayerNorm [60] in ViT. Re-purposing these methods to few-shot settings requires full backpropagation and mini-batch training. Despite having more parameters, ProLIP $_{\emptyset}$ is much faster and largely outperforms both baselines. Results are shown in Tab. 16.

13. Further analysis and discussion

Complementarity to other methods. We showed in Tab. 8 that ProLIP is complementary to other methods that learn different components for few-shot adaptation. Recently, Tang *et al.* [45] proposed interpreting CLIP few-shot adaptation methods from a unified perspective of logit bias. That is, every method learns a bias on top of the zero-shot CLIP logits. We detail here the bias learned by each of the two methods ProLIP was shown to be complementary to: TaskRes and Tip-Adapter-F, as well as the bias learned by ProLIP. TaskRes learns an element-wise adapter on top of t , the text-based frozen classifier. It writes:

$$\text{Logits}_{\text{TaskRes}} = \mathbf{v}^T(\mathbf{t} + \alpha \mathbf{r}) = \underbrace{\mathbf{v}^T \mathbf{t}}_{\text{zero-shot logits}} + \alpha \mathbf{v}^T \mathbf{r}. \quad (15)$$

The bias learned by TaskRes is thus a new linear probe trained on top of frozen visual features \mathbf{v} .

Tip-Adapter-F builds a cache model from the training features $\mathbf{F}_{\text{train}}$ and their labels $\mathbf{L}_{\text{train}}$. It writes:

$$\text{Logits}_{\text{Tip-Adapter-F}} = \underbrace{\mathbf{v}^T \mathbf{t}}_{\text{zero-shot logits}} + \alpha \phi(\mathbf{v}^T \mathbf{F}_{\text{train}}^T) \mathbf{L}_{\text{train}}. \quad (16)$$

	Base	New	H_{t1}	H_{t2}
CLIP	61.72	65.91	63.64	63.75
CoOp	71.96	61.26	65.58	66.18
CoCoOp	72.23	60.77	65.35	66.01
ProGrad	<u>73.29</u>	65.96	69.06	69.43
ProLIP $_{\emptyset}$	75.45	69.43	72.12	72.31

(a) Average over 11 datasets.

	Base	New	HM
CLIP	55.55	66.35	60.47
CoOp	61.77	62.51	62.14
CoCoOp	61.68	59.98	60.82
ProGrad	63.01	64.32	63.66
ProLIP $_{\emptyset}$	64.61	65.93	65.26

(e) StanfordCars

	Base	New	HM
CLIP	66.45	70.17	68.26
CoOp	71.48	65.57	68.40
CoCoOp	71.88	67.10	69.41
ProGrad	73.71	69.78	71.69
ProLIP $_{\emptyset}$	75.20	72.69	73.92

(i) SUN397

	Base	New	HM
	64.46	59.99	62.14
	65.49	57.70	61.35
	66.21	58.01	61.84
	66.96	60.04	63.23
	67.39	62.24	64.71

(b) ImageNet

	Base	New	HM
	64.10	70.92	67.34
	89.33	62.77	73.73
	88.07	66.26	75.62
	88.19	69.38	77.66
	89.42	72.34	79.98

(f) Flowers102

	Base	New	HM
	49.31	54.35	51.71
	67.71	43.92	53.28
	63.54	40.78	49.68
	66.90	53.06	59.18
	71.00	57.09	63.29

(j) DTD

	Base	New	HM
	72.43	68.14	70.22
	76.47	67.88	71.92
	75.98	70.43	73.10
	76.66	70.54	73.47
	76.56	68.63	72.38

(b) ImageNet

	Base	New	HM
	72.08	77.80	74.83
	97.60	59.67	74.06
	94.87	71.75	81.71
	95.92	72.46	82.56
	96.14	74.09	83.69

(f) Flowers102

	Base	New	HM
	53.24	59.90	56.37
	79.44	41.18	54.24
	77.01	56.00	64.85
	80.36	59.18	68.16
	81.44	60.23	69.25

(e) StanfordCars

	Base	New	HM
CLIP	69.36	75.35	72.23
CoOp	80.60	65.89	72.51
CoCoOp	79.74	76.86	78.27
MaPLe	80.82	78.70	79.75
ProLIP $_{\emptyset}$	82.22	77.29	79.68

(i) SUN397

(j) DTD

	Base	New	HM
	90.90	90.72	90.81
	94.38	87.48	90.80
	94.43	87.81	91.00
	94.47	90.84	92.46
	95.39	91.15	93.22

(c) Caltech101

	Base	New	HM
	81.48	82.15	81.81
	80.40	81.09	80.74
	79.77	77.68	78.71
	83.10	83.57	83.33
	82.39	84.47	83.42

(d) OxfordPets

	Base	New	HM
	39.26	43.62	41.33
	73.53	40.19	51.97
	83.63	40.95	54.98
	79.67	49.99	61.43
	88.16	66.69	75.94

(g) Food101

	Base	New	HM
	96.84	94.00	95.40
	98.00	89.81	93.73
	97.96	93.81	95.84
	97.74	94.36	96.02
	98.55	94.39	96.43

(k) EuroSAT

	Base	New	HM
	91.17	97.26	94.12
	93.67	95.29	94.47
	95.20	97.69	96.43
	95.43	97.76	96.58
	94.96	96.64	95.79

(l) UCF101

	Base	New	HM
	27.19	36.29	31.09
	40.44	22.30	28.75
	33.41	23.71	27.74
	37.44	35.61	36.50
	44.01	33.94	38.32

	Base	New	HM
	70.53	77.50	73.85
	84.69	56.05	67.46
	82.33	73.45	77.64
	83.00	78.66	80.77
	86.57	78.91	82.56

	Base	New	HM
	16		

Table 18. **Base-to-new generalization with ViT-B/16.** Per-dataset base, new, and harmonic mean accuracy of ProLIP $_{\emptyset}$ with $N = 16$ (except ‘CLIP’ which is zero-shot); cf. Tab. 5(b).

F_{train} is fine-tuned, thus the bias is based on intra-modal similarity measures (*i.e.*, similarities in the visual space).

For ProLIP, we fine-tune the projection matrix \mathbf{W}_o . Omitting b_o for simplicity, the logits can be written as:

$$\text{Logits}_{\text{ProLIP}} = \mathbf{x}_o^\top \mathbf{W}_o^\top \mathbf{t} = \underbrace{\mathbf{x}_o^\top \mathbf{W}_o^{(0)\top} \mathbf{t}}_{\text{zero-shot logits}} + \mathbf{x}_o^\top \mathbf{B}^\top \mathbf{t}. \quad (17)$$

That is, fine-tuning \mathbf{W}_o is equivalent to learning a matrix \mathbf{B} , initialized with $\mathbf{0}_{D \times D_o}$. Thus, the bias learned by ProLIP is a linear combination of the pre-projected features, trained to match the fixed text-based probe \mathbf{t} . In short, each of the three methods learn a different bias, and we hypothesis that the results of Tab. 8 reflect that these biases contain orthogonal knowledge learned during few-shot adaptation.

It is worth noting that we fixed the LR to 10^{-4} for all the datasets in these experiments. While the complementarity was shown for fixed hyperparameters across all datasets, ($\alpha = \beta = 1$ for Tip-Adapter-F and $\alpha = 0.1$ for TaskRes), increasing the LR to 10^{-2} lead to overfitting since the biases of TaskRes and Tip-Adapter-F are not regularized, which highlight again the advantage of ProLIP in stability across LRs.

Revisiting CLIP-Adapter [13] with ProLIP’s principles. Tab. 19 reports detailed results of CLIP-Adapter when varying its residual weight (α) and the learning rate (LR). Not only are the averaged results significantly worse than those of the Regularized Linear Adapter (RLA) variant and ProLIP $_\emptyset$, but CLIP-Adapter also exhibits high variance, especially in low-shot settings. Incorporating the ProLIP’s principles, RLA consistently improves performance while being much more stable. Our ProLIP $_\emptyset$ still achieves the best results.

Number of augmented views. Following the literature [23, 58], we apply RandomResizedCrop and RandomHorizontalFlip augmentations during training. As mentioned earlier, ProLIP can be applied on pre-computed visual embeddings (before the projection layer). We ablate the number of views in which the features are saved. Fig. 7 shows that average accuracy over 11 datasets increases with more views. Interestingly, ~ 10 views are sufficient to get results close to those with 300 views. In contrast, Lin et al. [31] showed that the gain saturates after more than two views for their cross-modal linear probe.

Visualization. We use UMAP to visualize EuroSAT test set feature manifolds, before and after 16-shot training (*i.e.*, zero-shot vs. ProLIP). The results are illustrated in Figs. 8a and 8b. We observe that the features are generally better clustered for ProLIP. Confusing categories like *Highway* or *Road*, *Permanent Crop Land* and *Pasture Land* exhibit remarkably better separation for our few-shot adapted model compared to zero-shot. This visualization hints that ProLIP

	Method	$N = 1$	2	4	8	16	Average
$\alpha = 0$	LR= 10^{-5}	17.92	30.80	44.39	55.41	63.02	42.31
	LR= 10^{-4}	39.17	50.45	59.91	66.78	71.74	57.61
	LR= 10^{-3}	41.79	51.78	60.04	66.41	71.14	58.23
	LR= 10^{-2}	39.36	45.45	49.47	52.34	53.28	47.98
	Average	34.56	44.62	53.45	60.24	64.80	51.53
$\alpha = 0.1$	LR= 10^{-5}	57.65	62.21	66.46	70.30	73.12	65.95
	LR= 10^{-4}	57.40	62.26	66.84	70.97	74.39	66.37
	LR= 10^{-3}	44.81	53.50	61.25	67.13	71.49	59.64
	LR= 10^{-2}	38.42	44.90	49.05	51.76	53.07	47.44
	Average	49.57	55.72	60.90	65.04	68.02	59.85
$\alpha = 0.3$	LR= 10^{-5}	63.39	66.62	69.39	71.88	73.69	68.99
	LR= 10^{-4}	60.26	64.28	68.23	71.96	75.12	67.97
	LR= 10^{-3}	50.77	58.05	63.86	68.77	72.74	62.84
	LR= 10^{-2}	37.55	44.37	49.22	52.07	54.69	47.58
	Average	52.99	58.33	62.68	66.17	69.06	61.85
$\alpha = 0.5$	LR= 10^{-5}	63.79	66.61	68.72	70.40	71.48	68.20
	LR= 10^{-4}	60.78	64.75	68.48	72.03	74.94	68.20
	LR= 10^{-3}	55.47	60.73	65.62	69.90	73.54	65.05
	LR= 10^{-2}	35.07	41.79	45.50	47.73	50.72	44.16
	Average	53.78	58.47	62.08	65.02	67.67	61.40
$\alpha = 0.7$	LR= 10^{-5}	63.18	64.96	66.01	66.57	66.88	65.52
	LR= 10^{-4}	61.32	65.19	68.69	71.75	74.02	68.19
	LR= 10^{-3}	56.98	61.63	66.15	70.41	74.05	65.84
	LR= 10^{-2}	36.73	41.80	43.91	46.28	47.87	43.32
	Average	54.55	58.40	61.19	63.75	65.71	60.72
$\alpha = 0.9$	LR= 10^{-5}	60.74	60.99	61.04	61.12	61.13	61.00
	LR= 10^{-4}	62.42	65.40	67.38	68.69	69.40	66.66
	LR= 10^{-3}	58.55	63.13	67.47	71.23	74.14	66.90
	LR= 10^{-2}	51.42	56.48	61.59	66.71	70.91	61.42
	Average	58.28	61.50	64.37	66.94	68.90	64.00
RLA, $\lambda = 1/N$	LR= 10^{-5}	63.23	65.56	68.08	70.90	73.44	68.24
	LR= 10^{-4}	63.41	65.80	68.27	70.91	73.35	68.35
	LR= 10^{-3}	63.38	65.82	68.30	70.99	73.55	68.41
	LR= 10^{-2}	63.35	65.78	68.29	70.99	73.57	68.40
	Average	63.34	65.74	68.24	70.95	73.48	68.35
ProLIP $_\emptyset$, $\lambda = 1/N$	LR= 10^{-5}	64.28	67.07	69.68	72.57	75.20	69.76
	LR= 10^{-4}	64.40	67.28	70.08	72.97	75.57	70.06
	LR= 10^{-3}	64.39	67.20	70.01	73.02	75.73	70.07
	LR= 10^{-2}	64.25	67.20	69.98	72.70	75.34	69.89
	Average	64.33	67.19	69.94	72.82	75.46	69.95

Table 19. **Improving CLIP-Adapter with ProLIP’s principles** results in the Regularized Linear Adapter (RLA) variant. We report classification accuracy (%) averaged over 11 datasets, 10 seeds, and 4 learning rates $\text{LR} \in \{10^{-5}, 10^{-4}, 10^{-3}, 10^{-2}\}$ for CLIP-Adapter with different α values, ProLIP $_\emptyset$ and RLA with $\lambda = 1/N$.

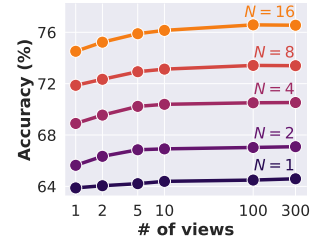


Figure 7. **Effect of augmented views.** Ablation of ProLIP using varying number of views and shots.

learns better feature manifolds in the few-shot classification setting.

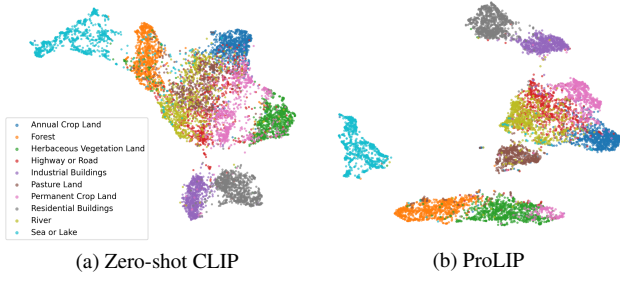


Figure 8. **Ablation and UMAP Visualization.** (a) and (b) UMAP of Zero-shot CLIP vs. ProLIP on EuroSAT, showing that some classes (e.g., ‘Pasture Land’, ‘Permanent Crop Land’, ‘Sea or Lake’, etc.) are better clustered with our method.

temp	$N = 1$	2	4	8	16
50	64.47	67.37	70.25	73.13	75.72
100	64.40	67.28	70.08	72.97	75.57
150	64.15	67.03	69.85	72.70	75.24

Table 20. **Effect of temperature (temp).** We report classification accuracy (%) of ProLIP $_{\phi}$ averaged over 11 datasets and 10 seeds for different temperature values. LR= 10^{-4} and $\lambda = 1/N$ for all datasets.

More few-shot settings & Full data training. Training on 32 shots, ProLIP $_{\phi}$ yields 77.79% average accuracy over 11 datasets and 10 seeds, better than lower-shot results (cf. Tab. 2b). Using full data for training, ProLIP $_{\phi}$ improves to 81.03% compared to 79.97% for TaskRes. Of note, Tip-adapter-F trains $N_{\text{data}} \times D$ parameters, thus 1.3B parameters for full ImageNet, which is not feasible. This also highlights the benefit of ProLIP for which the number of trainable parameters is not a function of the dataset size.

Effect of temperature. In all the experiments of the paper, we use the pretrained temperature value $\text{temp} = 1/\tau = 100$ (cf. Eq. (2)). Here we ablate this choice and show in Tab. 20 the performance of ProLIP $_{\phi}$ for $\text{temp} = 50$ and $\text{temp} = 150$. We observe that the performance is not highly affected, and that $\text{temp} = 50$ even outperforms the pretrained value. Studying in depth the effect of this parameter is left for future research.

14. ProLIP training details

The text encoder is fully frozen during training of ProLIP. The templates are similar to previous works [23, 58] for fair comparison, and are detailed in Tab. 21 for each dataset.

For training, only the weight matrix W_o in Eq. (1) is fine-tuned. Note that for ResNets, a bias term b_o exists while for ViTs no bias is added in pretraining. We stress that fine-tuning also the bias term for ResNets does not change the results, as most of the parameters are concentrated in the

Dataset	Template
Caltech101	“a photo of a {class}.”
StanfordCars	“a photo of a {class}.”
SUN397	“a photo of a {class}.”
DTD	“{class} texture.”
Eurosat	“a centered satellite photo of {class}.”
FGVCAircraft	“a photo of a {class}, a type of aircraft.”
Food101	“a photo of {class}, a type of food.”
Flowers102	“a photo of a {class}, a type of flower.”
OxfordPets	“a photo of a {class}, a type of pet.”
UCF101	“a photo of a person doing {class}.”
ImageNet	Ensemble of 7 templates:
ImageNet-A	“itap of a {class}.”, “a bad photo of the {class}.”,
ImageNet-V2	“a origami {}.”, “a photo of the large {class}.”,
ImageNet-R	“a {class} in a video game.”, “art of the {class}.”,
ImageNet-Sketch	“a photo of the small {class}.”

Table 21. **Dataset-specific templates.** Following the literature, all but ImageNet dataset and its variants use a single template.

weight matrix. In detail for ResNet-50, $W_o \in \mathbb{R}^{D \times D_o}$, where $D = 1024$ and $D_o = 2048$, this makes a total of $\sim 2M$ parameters, while $b_o \in \mathbb{R}^D$ has only 1024 parameters. Tab. 22 shows the number of trainable parameters in ProLIP for different backbones.

Backbone	$D \times D_o$	Parameters in W_o
ResNet-50	1024×2048	2.097M
ResNet-101	512×2048	1.049M
ViT-B/32	512×768	0.393M
ViT-B/16	512×768	0.393M

Table 22. **Number of trainable parameters per backbone.** It is the number of elements in the projection matrix $W_o \in \mathbb{R}^{D \times D_o}$.

15. Preliminaries

15.1. Zero-shot classification

We denote f and g the vision and text encoders of CLIP, respectively. During pretraining, CLIP learns a joint embedding space that pulls corresponding image-text representations closer together and pushes away dissimilar ones. At inference, given an image \mathbf{l} , one only needs the names of K candidate classes to perform *zero-shot classification*:

$$\hat{k} = \text{argmax}_k \mathbf{v}^T \mathbf{t}_k, \quad (18)$$

where $\mathbf{v} = \frac{f(\mathbf{l}; \theta_f)}{\|f(\mathbf{l}; \theta_f)\|_2}$, $\mathbf{t}_k = \frac{g(\mathbf{T}_k; \theta_g)}{\|g(\mathbf{T}_k; \theta_g)\|_2}$; θ_f and θ_g are the frozen parameters of f and g , respectively; \mathbf{T}_k is a text prompt describing the class k , e.g., “a photo of {class $_k$ }”.

15.2. Few-shot classification

Given a set of N labeled samples from each of the K classes, research has been carried out to efficiently adapt CLIP using this set. All existing research in this direction can be gathered in three main avenues (see Fig. 1).

Prompt Tuning. It parameterizes the prompt template, *i.e.*, $T_k = [\mathbf{w}]_1[\mathbf{w}]_2 \dots [\mathbf{w}]_M[\text{class}_k]$, where $[\mathbf{w}]_1, [\mathbf{w}]_2, \dots$, and $[\mathbf{w}]_M$ are learned while keeping f and g frozen. Prompt tuning adapts CLIP “indirectly” on the classifier side, *i.e.*, the text embeddings are derived from the learned prompts.

Adapters. They learn a multi-layer perceptron (MLP) h_θ with a residual connection α on top of the frozen visual features \mathbf{v} , *i.e.*, $\mathbf{v} := \alpha\mathbf{v} + (1 - \alpha)h_\theta(\mathbf{v})$, or on top of the frozen text features \mathbf{t} , *i.e.*, $\mathbf{t} := \alpha\mathbf{t} + (1 - \alpha)h_\theta(\mathbf{t})$, or both.

Linear probing. It trains a linear classifier $\mathbf{W} \in \mathbb{R}^{K \times D}$ on top of the frozen visual features, D being the embedding space dimension. Matrix \mathbf{W} can be initialized with text embeddings \mathbf{t}_k . Since the classifier is directly tuned, linear probing restricts CLIP to K classes after adaptation and cannot be applied in open-class setting.

15.3. CLIP architecture

CLIP adopts a transformer architecture [46] for the text encoder, but the vision encoder may be either a ResNet [17] or a Vision Transformer (ViT) [10]. We detail both architectures below and later elaborate on our unified method applicable to both architectures regardless of their intrinsic differences.

ResNet. CLIP replaces the global average pooling layer in ResNet with an attention pooling layer. The output of the multi-head attention layer is then projected to the shared latent space using a linear layer. Thus, f can be written as $f = f_2 \circ f_1$, where f_1 represents all the layers up to the attention pooling (included), and f_2 represents the linear projection head. Given an image \mathbf{I} :

$$\mathbf{x}_o = f_1(\mathbf{I}), \quad \mathbf{v} = f_2(\mathbf{x}_o) = \mathbf{W}_o \mathbf{x}_o + \mathbf{b}_o, \quad (19)$$

with $\mathbf{x}_o \in \mathbb{R}^{D_o}$ the output of the attention pooling layer, $\mathbf{W}_o \in \mathbb{R}^{D \times D_o}$ the projection matrix and \mathbf{b}_o a bias term.

ViT. The transformer encoder consists of multiple residual attention blocks. Each block has two main components: a multi-head self-attention and a feed-forward neural network (MLP), with residual connections. The output of the last residual attention block is projected to the latent space using a trainable matrix. Thus, f can be written as $f = f_2 \circ f_1$, where f_1 represents all the layers up to the last residual attention block (included), and f_2 represents the projection matrix. Given an image \mathbf{I} :

$$\mathbf{x}_o = f_1(\mathbf{I}), \quad \mathbf{v} = f_2(\mathbf{x}_o) = \mathbf{W}_o \mathbf{x}_o, \quad (20)$$

where no bias term is included, unlike Eq. (19).

Similarly on the text side, the embeddings are projected into the shared latent space using a linear layer.

Dataset	Method	$N = 1$	2	4	8	16
CLIP (0-shot)			60.35			
ImageNet	CoOp [63]	61.19	61.58	62.22	62.87	63.70
	PLOT [6]	60.46	60.73	61.79	62.48	63.08
	KgCoOp [52]	60.90	61.44	62.00	62.20	62.43
	ProGrad [64]	61.58	62.14	62.59	63.04	63.54
	CLIP-Adapter [13]	59.82	59.94	59.97	59.98	61.31
	Tip-Adapter-F [58]	60.59	61.42	62.12	63.41	65.06
Tip-Adapter-F* [58]						
SUN397	Standard LP [36]	22.21	31.96	41.48	49.49	56.04
	LP++ [23]	61.18	61.56	62.55	63.76	64.73
	ProLIP	61.28	61.79	62.38	63.30	64.31
	CLIP (0-shot)	58.85				
	CoOp [63]	61.79	63.32	65.79	67.89	70.15
	PLOT [6]	62.53	63.87	65.85	67.83	69.90
KgCoOp [52]						
DTD	ProGrad [64]	62.79	64.12	66.32	68.33	70.18
	CLIP-Adapter [13]	60.78	61.79	63.84	66.26	67.66
	Tip-Adapter-F [58]	61.02	62.15	63.86	67.25	70.94
	Tip-Adapter-F* [58]	62.58	63.79	65.49	67.43	69.25
	Standard LP [36]	32.56	43.77	54.49	61.83	67.03
	LP++ [23]	62.47	64.65	67.28	69.34	71.23
ProLIP						
Caltech101	63.44	65.16	67.39	69.31	71.31	
	CLIP (0-shot)	42.69				
	CoOp [63]	42.31	47.13	54.06	59.21	63.67
	PLOT [6]	45.82	51.32	55.67	61.38	65.29
	KgCoOp [52]	45.46	50.01	53.37	58.38	62.71
	ProGrad [64]	44.19	50.41	54.82	60.31	63.89
CLIP-Adapter [13]						
UCF101	43.49	44.49	48.95	57.52	62.97	
	Tip-Adapter-F [58]	46.92	48.50	57.16	62.38	65.23
	Tip-Adapter-F* [58]	47.68	52.24	56.09	61.05	65.04
	Standard LP [36]	29.63	41.19	51.72	58.78	64.56
	LP++ [23]	46.97	52.44	57.75	62.42	66.40
	ProLIP	50.21	54.75	59.30	64.19	68.02
CLIP (0-shot)						
Flowers102	CoOp [63]	87.06	89.14	90.00	91.00	91.77
	PLOT [6]	89.41	90.22	90.69	91.55	92.17
	KgCoOp [52]	88.24	88.85	89.89	90.32	90.93
	ProGrad [64]	88.34	89.01	90.13	90.76	91.67
	CLIP-Adapter [13]	87.69	89.37	90.21	91.33	92.10
	Tip-Adapter-F [58]	87.35	88.17	89.49	90.54	92.10
Tip-Adapter-F* [58]						
Caltech101	88.68	89.36	90.40	91.62	92.63	
	Standard LP [36]	68.88	78.41	84.91	88.70	91.14
	LP++ [23]	88.56	89.53	90.87	91.84	92.73
	ProLIP	89.25	89.80	91.47	92.37	93.44
	CLIP (0-shot)	61.80				
	CoOp [63]	62.80	65.62	68.69	72.57	76.39
PLOT [6]						
UCF101	63.22	66.49	70.12	74.63	77.39	
	KgCoOp [52]	64.37	64.91	68.41	69.86	71.73
	ProGrad [64]	65.13	66.57	69.80	73.01	75.76
	CLIP-Adapter [13]	64.25	66.68	69.77	73.90	77.26
	Tip-Adapter-F [58]	64.28	65.48	67.61	72.05	77.30
	Tip-Adapter-F* [58]	65.50	68.55	70.55	74.25	76.83
Standard LP [36]						
Flowers102	40.80	51.71	61.64	68.47	73.38	
	LP++ [23]	65.41	69.20	71.68	74.86	77.46
	ProLIP	67.88	70.07	73.51	77.06	79.79
	CLIP (0-shot)	65.98				
	CoOp [63]	69.00	78.47	85.34	91.68	94.47
	PLOT [6]	71.09	81.22	87.61	92.60	95.18
KgCoOp [52]						
Caltech101	68.73	69.63	76.51	80.71	84.48	
	ProGrad [64]	72.16	79.55	84.56	91.73	94.10
	CLIP-Adapter [13]	66.86	69.71	77.42	87.20	91.16
	Tip-Adapter-F [58]	67.73	68.18	71.17	84.11	93.02
	Tip-Adapter-F* [58]	78.46	85.14	88.53	92.33	94.26
	Standard LP [36]	56.98	73.40	84.38	91.81	95.05
LP++ [23]						
Flowers102	78.21	84.69	89.56	92.61	94.26	
	ProLIP	75.33	81.95	88.34	92.68	94.92

Table 23. **Comparison to state-of-the-art methods.** Average classification accuracy (%) and standard deviation over 10 tasks for 11 benchmarks. Best values are highlighted in bold.

Dataset	Method	$N = 1$	2	4	8	16
<i>StanfordCars</i>	CLIP (0-shot)			55.78		
	CoOp [63]	57.00	58.96	62.81	68.40	72.87
	PLOT [6]	57.47	59.89	63.49	68.75	73.86
	KgCoOp [52]	57.19	58.94	59.85	61.42	62.99
	ProGrad [64]	58.63	61.23	65.02	69.43	72.76
	CLIP-Adapter [13]	56.67	57.94	61.13	65.43	70.24
	Tip-Adapter-F [58]	57.24	58.12	59.34	64.25	71.38
	Tip-Adapter-F* [58]	57.85	60.55	64.22	68.75	74.19
	Standard LP [36]	22.94	35.48	47.49	59.34	69.11
	LP++ [23]	57.20	59.95	63.44	67.81	72.33
	ProlIP	58.72	61.71	65.68	70.64	75.64
<i>FGVCAircraft</i>	CLIP (0-shot)			17.07		
	CoOp [63]	12.50	17.59	21.27	26.85	31.20
	PLOT [6]	17.75	19.55	22.26	26.70	32.09
	KgCoOp [52]	18.61	18.93	21.16	22.80	24.10
	ProGrad [64]	18.41	20.51	23.65	26.98	30.47
	CLIP-Adapter [13]	18.56	19.18	21.00	23.76	33.37
	Tip-Adapter-F [58]	18.23	19.12	20.55	23.60	30.37
	Tip-Adapter-F* [58]	19.08	20.79	23.99	30.58	36.16
	Standard LP [36]	12.66	16.92	21.11	26.53	32.42
	LP++ [23]	19.69	21.58	24.22	27.73	31.73
	ProlIP	19.74	22.68	27.08	33.20	39.90
<i>EuroSAT</i>	CLIP (0-shot)			36.22		
	CoOp [63]	40.36	56.15	66.13	77.02	82.59
	PLOT [6]	44.22	64.19	69.37	78.84	81.76
	KgCoOp [52]	43.86	52.92	59.51	63.23	64.04
	ProGrad [64]	49.37	65.22	69.57	78.44	82.17
	CLIP-Adapter [13]	43.00	48.60	59.15	69.92	75.38
	Tip-Adapter-F [58]	47.63	57.62	69.30	75.22	78.59
	Tip-Adapter-F* [58]	49.27	65.66	70.72	74.66	78.73
	Standard LP [36]	48.29	56.81	64.99	74.56	80.29
	LP++ [23]	57.23	61.65	68.67	75.86	80.53
	ProlIP	57.95	70.03	76.48	81.81	85.81
<i>OxfordPets</i>	CLIP (0-shot)			85.75		
	CoOp [63]	86.27	86.33	85.34	87.85	88.68
	PLOT [6]	87.15	87.23	88.03	88.38	88.23
	KgCoOp [52]	87.51	87.51	88.04	88.59	89.28
	ProGrad [64]	88.34	87.88	88.59	88.87	89.39
	CLIP-Adapter [13]	85.46	86.37	87.21	87.95	88.33
	Tip-Adapter-F [58]	85.70	86.05	86.40	87.66	89.08
	Tip-Adapter-F* [58]	86.05	86.49	87.19	87.89	88.26
	Standard LP [36]	30.62	42.64	55.60	67.32	76.23
	LP++ [23]	84.24	85.74	86.94	87.71	88.38
	ProlIP	85.46	86.17	87.05	88.15	89.17
<i>Food101</i>	CLIP (0-shot)			77.35		
	CoOp [63]	75.58	77.49	77.93	78.92	79.21
	PLOT [6]	77.46	77.72	78.23	78.40	78.86
	KgCoOp [52]	77.20	78.04	77.97	78.39	78.73
	ProGrad [64]	78.36	78.01	78.38	79.11	79.51
	CLIP-Adapter [13]	76.93	77.22	77.64	77.97	78.45
	Tip-Adapter-F [58]	77.53	77.53	77.82	78.26	78.99
	Tip-Adapter-F* [58]	77.58	77.36	77.78	78.17	78.72
	Standard LP [36]	31.59	44.60	56.13	64.45	70.97
	LP++ [23]	76.61	77.22	77.79	78.53	78.88
	ProlIP	77.06	77.61	77.74	78.37	79.21

Table 24. Comparison to state-of-the-art methods (Continued).

Average classification accuracy (%) and standard deviation over 10 tasks for 11 benchmarks. Best values are highlighted in bold.